Acta Neuropathol (2004) 107: 149–158
DOI 10.1007/s00401-003-0791-1

REGULAR PAPER

Shinsuke Kato · Yusuke Saeki · Masashi Aoki · Makiko Nagai · Aya Ishigaki · Yasuto Itoyama · Masako Kato
Kohtaro Asayama · Akira Awaya · Asao Hirano · Eisaku Ohama

Histological evidence of redox system breakdown caused by superoxide dismutase 1 (SOD1) aggregation is common to SOD1-mutated motor neurons in humans and animal models

Received: 8 July 2003 / Revised: 10 October 2003 / Accepted: 13 October 2003 / Published online: 27 November 2003

Abstract Living cells produce reactive oxygen species (ROSs). To protect themselves from these ROSs, the cells have developed both an antioxidant system containing superoxide dismutase 1 (SOD1) and a redox system including peroxiredoxin2 (Prx2, thioredoxin peroxidase) and glutathione peroxidase1 (GPx1): SOD1 converts superoxide radicals into hydrogen peroxide (H_2O_2), and H_2O_2 is then converted into harmless water (H_2O) and oxygen (O_2) by Prx2 and GPx1 that directly regulate the redox system. To clarify the biological significance of the interaction of the redox system (Prx2/GPx1) with SOD1 in SOD1-mutated motor neurons in vivo, we produced an affinity-purified rabbit antibody against Prx2 and investigated the immunohistochemical localization of Prx2 and GPx1 in neuronal Lewy body-like hyaline inclusions (LBHIs) in the spinal cords of familial amyotrophic lateral sclerosis (FALS) patients with a two-base pair deletion at codon 126 and an Ala→Val substitution at codon 4 in the SOD1 gene, as well as in transgenic rats expressing human SOD1 with H46R and G93A mutations. The LBHIs in motor neurons from the SOD1-mutated FALS patients and transgenic rats showed identical immunoreactivities for Prx2 and GPx1: the reaction product deposits with the antibodies against Prx2 and GPx1 were localized in the LBHIs. In addition, the localizations of the immunoreactivities for SOD1 and Prx2/GPx1 were similar in the inclusions: the co-aggregation of Prx2/GPx1 with SOD1 in neuronal LBHIs in mutant SOD1-related FALS patients and transgenic rats was evident. Based on the fact that Prx2/GPx1 directly regulates the redox system, such co-aggregation of Prx2/GPx1 with SOD1 in neuronal LBHIs may lead to the breakdown of the redox system itself, thereby amplifying the mutant SOD1-mediated toxicity in mutant SOD1-linked FALS patients and transgenic rats expressing human mutant SOD1.

Keywords Peroxiredoxin 2 · Glutathione peroxidase 1 · Redox system · Superoxide dismutase 1 · Familial amyotrophic lateral sclerosis

S. Kato (✉) · Y. Saeki · E. Ohama
Department of Neuropathology,
Institute of Neurological Sciences, Faculty of Medicine,
Tottori University,
Nishi-cho 36-1, 683-8504 Yonago, Japan
Tel.: +81-859-348034, Fax: +81-859-348289,
e-mail: kato@grape.med.tottori-u.ac.jp

M. Aoki · M. Nagai · A. Ishigaki · Y. Itoyama
Department of Neuroscience, Division of Neurology,
Tohoku University Graduate School of Medicine, Sendai, Japan

M. Kato
Division of Pathology, Tottori University Hospital,
Yonago, Japan

K. Asayama
Department of Pediatrics,
University of Occupational and Environmental Health,
Kitakyushu, Japan

A. Awaya
Japan Science and Technology Corporation,
Tachikawa, Japan

A. Hirano
Division of Neuropathology,
Department of Pathology, Montefiore Medical Center,
Bronx, New York, USA

Introduction

Living cells produce reactive oxygen species (ROSs) during physiological processes and in response to external stimuli such as ultraviolet radiation. To protect itself from potentially destructive ROSs, each cell of living organisms has developed a sophisticated antioxidant enzyme defense system. In this system, there are two groups of enzymes: the enzymes of the first group convert superoxide radicals into hydrogen peroxide (H_2O_2), and the enzymes of the second group convert H_2O_2 into harmless water (H_2O) and oxygen (O_2). For the first antioxidant enzyme group, three isoforms of superoxide dismutase (SOD) [EC 1.15.1.1] have been identified: SOD1, SOD2, and SOD3 [9]. In the second enzyme group, the peroxiredoxin (Prx) and glutathione peroxidase (GPx) families, as well as catalase localized within peroxisomes have been identified. Unlike

SOD and catalase, enzymes of the Prx and GPx families require secondary enzymes and cofactors to function at high efficiency. In particular, the enzymes of the Prx- and GPx-families are considered to play a role in directly controlling the redox system. In general, the redox system regulates versatile control mechanisms in signal transduction and gene expression [29]. In mammalian cells, this redox signal transduction is linked to systems such as cellular differentiation, immune response, growth control, and apoptosis [10].

Peroxiredoxin2 (Prx2) is a novel organ-specific antioxidative enzyme that is mainly expressed in mammalian brain [23]. This protein is a member of Prx family, whose members possess reactive cysteine residues [23]. Prx2 requires thioredoxin reductase (TR) as a secondary enzyme as well as thioredoxin and NADPH as cofactors to function at high efficiency; the activity of Prx2 in the thioredoxin/TR/NADPH system is over five times higher than that of Prx2 by itself [5]. In this milieu, Prx2 is also called thioredoxin peroxidase 1 (thioredoxin-dependent peroxide reductase 1) or thiol-specific antioxidant [4, 5, 6]. In addition to controlling the intracellular content of H_2O_2, Prx2 directly regulates the redox signals of the thioredoxin/TR/NADPH system, because alone the secondary enzyme and cofactors (i.e., thioredoxin/TR/NADPH) can not directly regulate the redox system and can not act on H_2O_2. Cytosolic GPx [EC 1.11.1.9], a classical selenium-dependent isoform (also assigned as GPx1), was first described as an enzyme that protects hemoglobin from oxidative degradation in red blood cells [25]. The GPx family is composed of at least four GPx isoforms in mammals [7]. Among them, GPx1 is considered as the major enzyme responsible for removing intracytoplasmic H_2O_2. Like Prx2, GPx1 needs glutathione reductase (GR) as a secondary enzyme as well as glutathione and NADPH as cofactors to work at high efficiency, and this process is also one of the redox signals in living cells [21, 24]. Therefore, Prx2 and GPx1 directly control the redox system.

Approximately 20% of the cases of familial amyotrophic lateral sclerosis (FALS) are caused by a mutant SOD1 [15, 17, 18]. SOD1 is thought to be an essential component of neuronal Lewy body-like hyaline inclusions (LBHIs): neuronal LBHIs in affected anterior horn cells are morphological hallmarks of SOD1-mutated motor neurons of FALS patients [3, 11, 12, 13, 14, 15, 16, 17, 18, 30]. To cope with destructive ROSs, even SOD1-mutated motor neurons induce mutant and wild-type SOD1 as well as Prx2 and GPx1. Considering that Prx2 and GPx1 interact not only with wild-type SOD1 but also with mutant SOD1, the interaction of Prx2/GPx1 with SOD1 has been suggested to contribute to mutant SOD1 aggregation toxicity: Prx2/GPx1 possibly aggregate as LBHIs in SOD1-mutated motor neurons. Furthermore, the aggregation of Prx2/GPx1 might affect the intracytoplasmic redox regulation and amplify mutant SOD1-mediated toxicity. To clarify the biological significance of the interaction of Prx2/GPx1 (redox system) with SOD1 in SOD1-mutated motor neurons in vivo, we first produced an antibody against Prx2, and analyzed the characteristic expressions of both Prx2 and GPx1 in neuronal LBHIs in SOD1-mutated motor neurons of humans and animal models.

Materials and methods

Preparation of polyclonal antibody against Prx2

A synthetic peptide corresponding to the C-terminal region of Prx2 (amino acids 184–198: NH_2-KPNVDDSKEYFSKHN-COOH) with or without conjugation to human serum albumin (HSA) at the carboxyl end was supplied by Peptide Institute (Osaka, Japan). This amino acid sequence is homologous with those of the C-terminal region of the human, rat or mouse Prx2. The polyclonal antibody preparation was carried out according to the method of Kato et al. [16]. To prepare immunogen, 6 mg synthesized Prx2 peptide was conjugated with 6 mg keyhole limpet hemocyanin (KLH) in the presence of 50 mM 1-ethyl-3-(3-dimethylaminopropyl) carbodiimide-HCl (Pierce Chemical Co., Rockford, IL) and 2.5 mM *N*-hydroxysulfosuccinimide (Pierce) in 3 ml phosphate-buffered saline (PBS) pH 7.4 for 1 h at room temperature. The reaction was terminated by adding 2-mercaptoethanol to the concentration of 20 mM and dialyzed against PBS for 24 h. To raise polyclonal antibodies, 500 µg of the immunogen in 50% Freund's complete adjuvant was inoculated intradermally into a rabbit at 20 skin sites; four booster inoculations of 500 µg immunogen in 50% Freund's incomplete adjuvant were given at 10, 17, 24 and 31 days after the first inoculation. The serum was taken 10 days after the final immunization. The IgG fraction in the antiserum against the immunogen, the hapten-conjugated KLH, was purified by absorption on a protein G-Sepharose gel column (Pharmacia Biotech, Uppsala, Sweden). Subsequently, the antibodies were further purified on an affinity column of immobilized KLH conjugated with the synthetic Prx2 peptide, as described previously [16].

Enzyme-linked immunosorbent assay

Noncompetitive ELISA was carried out according to the method described by Kato et al. [16]. Each well of a 96-well microtiter plate was coated with 100 µl of 5 µg/ml immunogen in 5 mM sodium carbonate buffer (pH 9.6) and incubated for 60 min. This was followed by triplicate washing with PBS containing 0.05% Tween 20 (buffer A). Each well was blocked with 0.5% gelatin for 60 min and then washed three times with buffer A. Antibody solutions (100 µl) at the concentrations indicated in Fig. 1 (horizontal line) were added to each well and incubated for 60 min. The wells were then washed three times with buffer A. The binding of the horseradish peroxidase-conjugated secondary antibody (Wako Pure Chemical Industries, Osaka, Japan) to the primary antibody was visualized with 2, 2'-azino-bis-(3-ethylbenzothiazoline-6-sulfonate)-$(NH_3)_2$. The reaction was terminated with 1 M sulfuric acid, and the absorbance at 415 nm was read on a micro-ELISA plate reader (Tecan, Hombrechtikon, Switzerland).

Tissue collection

Histochemical and immunohistochemical studies were performed on archival, buffered 10% formalin-fixed, paraffin-embedded tissues obtained at autopsy from five FALS patients who were members of two different families. The main clinicopathological characteristics of the FALS patients are summarized in Table 1, and have been reported previously [12, 13, 20, 22, 28, 30, 31]. SOD1 analysis revealed that the members of the Japanese Oki family had a two-base pair deletion at codon 126 (frame-shift 126 mutation) [12] and the American C family members had an Ala→Val substitution at codon 4 (A4V) [30]. As human controls, we examined autopsy specimens of the spinal cord from 20 neurologically and neuropathologically normal individuals (11 male, 9 females; aged 37–75 years).

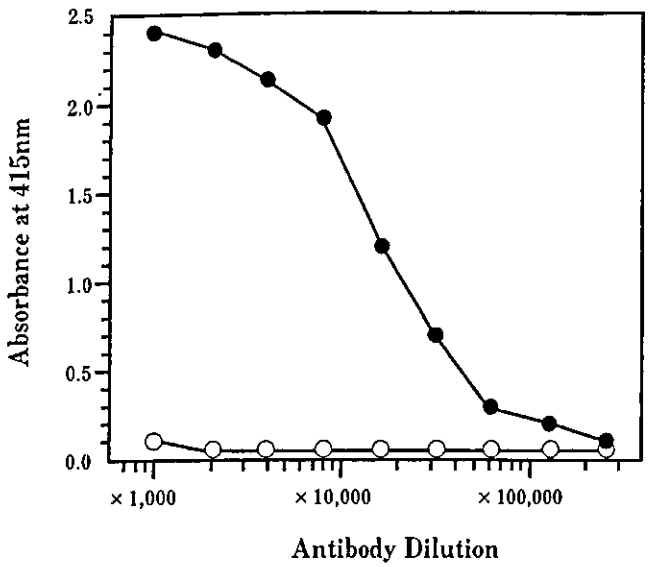

Fig. 1 Specificity of antibody against Prx2. The immunoreactivity of the antibody to HSA-conjugated Prx2 peptide (*solid circles*) and native HSA (*open circles*) was determined by noncompetitive ELISA. The anti-Prx2 antibody recognizes the HSA-conjugated Prx2 peptide, but does not react with HAS (*Prx2* peroxiredoxin2, *ELISA* enzyme-linked immunosorbent assay, *HAS* human serum albumin)

Histochemical and immunohistochemical studies were also carried out on specimens from transgenic rats with the H46R and G93A types of mutations (three rats of each type). The H46R rats used in this study were a transgenic line (H46R-4) in which the level of human SOD1 with the H46R mutation was 6 times the level of that of endogenous rat SOD1 [27]. The G93A rats were a transgenic line (G93A-39) in which the level of human SOD1 with the G93A mutation was 2.5 times the level of endogenous rat SOD1 [27]. These rats were killed at an age of over 180 days; an age corresponding to an advanced stage of disease in these strains. The detailed clinical signs and pathological characteristics of the neuronal LBHIs of the H46R and G93A rats have been demonstrated previously [27]. As rat controls, we investigated the spinal cord specimens of three age-matched littermates of H46R and G93A rats and five age-matched normal Sprague-Dawley rats. Rats were anesthetized with sodium pentobarbital (0.1 ml/100 g body weight). After perfusion of the rats via the aorta with physiological saline at 37°C, they were fixed by perfusion with 4% paraformaldehyde in 0.1 M cacodylate buffer (pH 7.3). The spinal cords were removed and then postfixed in the same solution.

Histochemistry and immunohistochemistry

After fixation, the specimens were embedded in paraffin, cut into 6-μm-thick sections, and examined by light microscopy. Spinal cord sections were stained by the following histochemical methods: hematoxylin and eosin (HE), Klüver-Barrera, Holzer, phosphotungstic acid-hematoxylin, periodic acid-Schiff, alcian blue, Masson's trichrome, Mallory azan and Gallyas-Braak stains. Representative paraffin sections were used for immunohistochemical assays. The following primary antibodies were utilized: an affinity-purified rabbit antibody against Prx2 (concentration: 1 μg/ml), a polyclonal antibody to GPx1 [diluted 1:2,000 in 1% bovine serum albumin-containing phosphate-buffered saline (BSA-PBS), pH 7.4] [2], and a polyclonal antibody to human SOD1 (diluted 1:10,000 in 1% BSA-PBS, pH 7.4) [1]. Sections were deparaffinized, and endogenous peroxidase activity was quenched by incubation for 30 min with 0.3% H_2O_2. The sections were then washed in PBS. Normal sera homologous with secondary antibody was used as a blocking reagent. Tissue sections were incubated with the primary antibodies for 18 h at 4°C. PBS-exposed sections served as controls. As a preabsorption test, some sections were incubated with the anti-Prx2 antibody that had been preabsorbed with an excess amount of the synthetic Prx2 peptide. Bound antibodies were visualized by the avidin-biotin-immunoperoxidase complex (ABC) method using the appropriate Vectastain ABC Kit (Vector Laboratories, Burlingame, CA) and 3,3'-diaminobenzidine tetrahydrochloride (DAB; Dako, Glostrup, Denmark) as chromogen.

Results

We successfully produced an affinity-purified rabbit antibody against Prx2 peptide (amino acids 184–198; although this amino acid sequence is homologous with that of each C-terminal region of the human, rat, mouse, Chinese hamster or Bos Taurus Prx2, this peptide does not share homology with other members of the Prx family or any other peptide sequence in GenomeNet), and applied it to stain of paraffin sections from both humans and rats. This anti-Prx2 antibody recognized the HSA-conjugated Prx2 peptide, but did not react with HSA (Fig. 1).

Analysis of the essential changes of five cases of FALS revealed a subtype of FALS with posterior column involvement (PCI). This subtype is characterized by the degeneration of the middle root zones of the posterior column, Clarke nuclei, and the posterior spinocerebellar tracts, in addition to spinal cord motor neuron lesions. A long-term surviving patient with a clinical course of 11 years

Table 1 Characteristics of five FALS cases (*FALS* familial amyotrophic lateral sclerosis, *SOD* superoxide dismutase, *LBHI* Lewy body-like hyaline inclusion, *2-bp* two-base pair, *PCI* posterior column involvement type, + detected, *ND* not determined, *As* asphyxia, *IH* intraperitoneal hemorrhage, *RD* respiratory distress, *Pn* pneumonia)

Case	Age (years)	Sex	Cause of Death	FALS Duration	SOD1 mutation	FALS subtype	Neuronal LBHI
Japanese Oki family							
1	46	F	As	18 months	2-bp deletion (126)	PCI	+
2	65	M	IH	11 years	2-bp deletion (126)	PCI and degeneration of other systems	+
American C family							
3	39	M	RD	7 months	A4V	PCI	+
4	46	M	Pn	8 months	A4V	PCI	+
5	66	M	Pn	1 year	ND	PCI	+

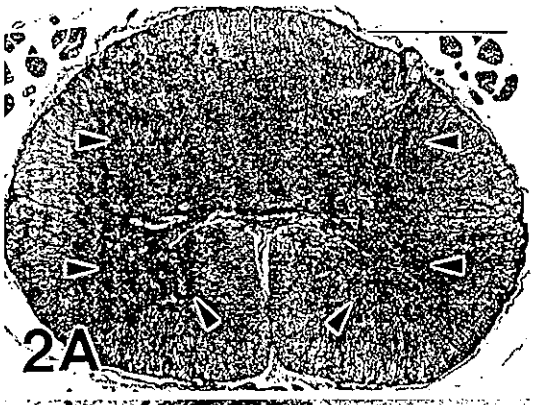

2A

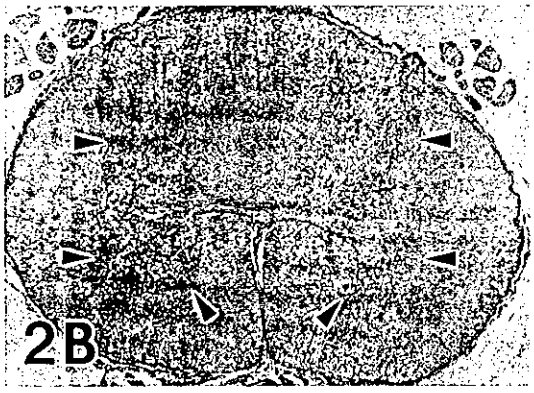

2B

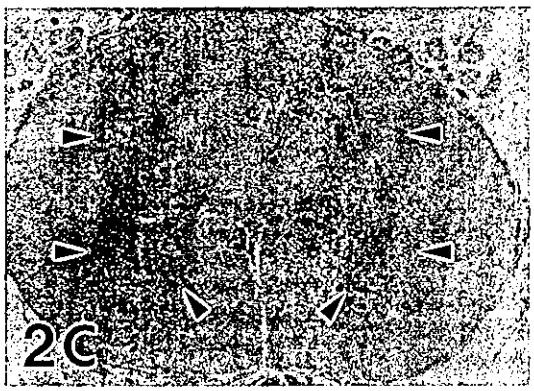

2C

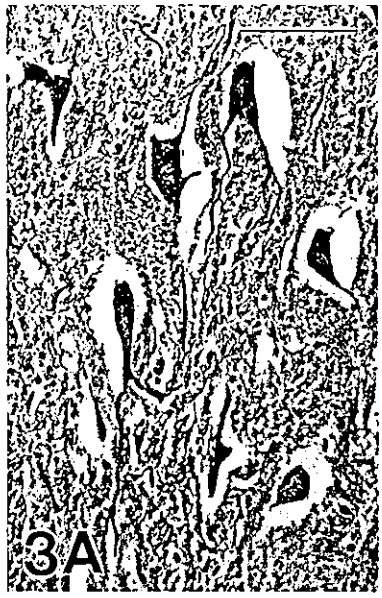

3A

3C

3B

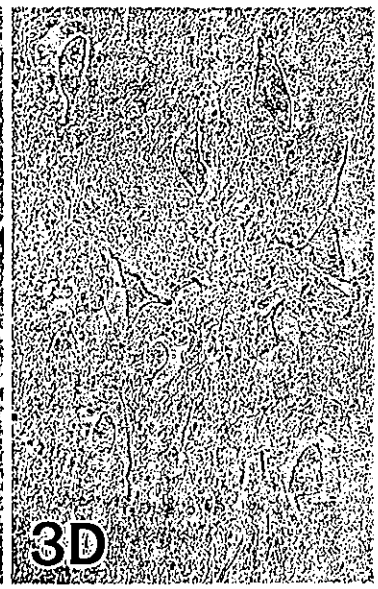

3D

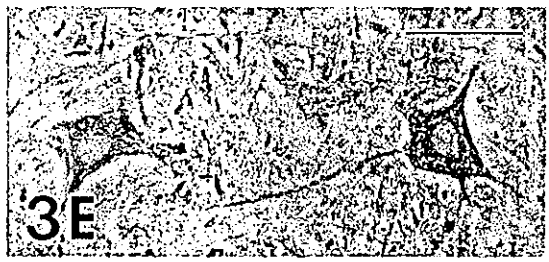

3E

3F

◀ Fig. 2 Serial transverse sections through the lumbar segments of the normal human spinal cords. A Light microscopic preparation stained with HE. B, C Immunostaining for GPx1 (B) and Prx2 (C). GPx1 and Prx2 immunoreactivities are found diffusely in the neuropil with considerably less intensity (*arrowheads*). No counterstaining (*HE* hematoxylin and eosin, *GPx1* glutathione peroxidase1, *Prx2* peroxiredoxin2). *Bar* A (also for B, C) 2 mm

Fig. 3 Detection of Prx2 and GPx1 in the normal motor neurons of the human spinal cord. A–D Serial sections. A Staining with HE. B Immunostaining with the antibody against GPx1, showing GPx1-positive neurons. C Immunostaining with the antibody to Prx2. Immunoreactivity is identified in most of the neurons. Thus, most of the normal motor neurons in the spinal cord co-express both GPx1 (B) and Prx2 (C), although their staining intensities in neurons vary. D Immunostaining with anti-Prx2 antibody pretreated with an excess of the synthetic Prx2 peptide. No immunoreaction products are observed in the motor neurons and neuropil. E GPx1 immunostaining of the neuronal cytoplasm and proximal dendrites is observed, but no intranuclear localization is seen. F Prx2 immunostaining of the neuronal cytoplasm and proximal dendrites is observed, and a nucleus of the neuron is also immunostained by the anti-Prx2 antibody. B–F No counterstaining (*HE* hematoxylin and eosin, *GPx1* glutathione peroxidase1, *Prx2* peroxiredoxin2). *Bars* A (also for B–D) 100 μm; E, F 50 μm

(case 2 in Table 1) showed multisystem degeneration in addition to the features of FALS with PCI. Neuronal Lewy body-like hyaline inclusions (LBHIs) were present in all five FALS cases. As observed in HE preparations, the neuronal LBHIs in the FALS patients were essentially identical to those in the H46R and G93A transgenic rats; the inclusions were round eosinophilic or paler inclusions and often showed eosinophilic cores with pale peripheral halos. In mutant SOD1-linked FALS patients, the neuronal LBHIs were generally composed of eosinophilic cores with pale peripheral halos and sometimes showed ill-defined forms that consisted of obscure eosinophilic materials. In H46R and G93A transgenic rats, the intracytoplasmic LBHIs with cores and halos were less frequently observed and round or sausage-like LBHIs, which were though to be intradendritic LBHIs, were often seen in the neuropil, although these round or sausage-like LBHIs in the neuropil were not remarkable in the human FALS patients. Histochemically, most of the neuronal LBHIs in the H46R and G93A transgenic rats were argyrophilic in Gallyas-Braak stain, and they were generally blue to violet after Masson's trichrome or Mallory azan staining, similar to the histochemical findings of the neuronal LBHIs of the human FALS patients. The spinal cords of normal individuals in both humans and rats did not exhibit any distinct histopathological alterations.

When control and representative paraffin sections were incubated with PBS alone (i.e., no primary antibody), no staining was detected. Prx2 immunoreactivity in normal spinal cords was identified in almost all neurons. In addition, Prx2-immunostaining was found throughout the neuropil with considerably lower intensity (Fig. 2A, C). With respect to the intracellular localization of Prx2, immunostaining of the neuronal cytoplasm and proximal dendrites was specifically observed (Fig. 3A, C). Additionally, the nuclei of some neurons were immunostained by the anti-Prx2 antibody, albeit the staining of positively stained nuclei varied (Fig. 3F). Incubation of sections with anti-Prx2 antibody that had been pretreated with an excess of the synthetic Prx2 produced no staining (Fig. 3D).

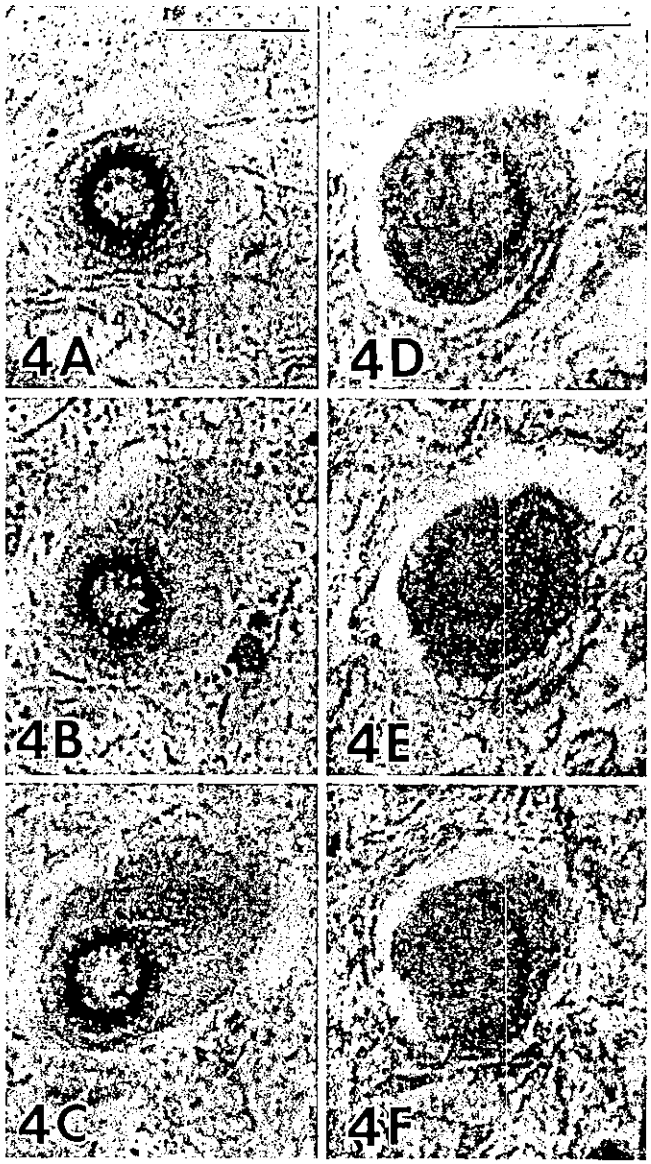

Fig. 4A–C Serial sections of a typical LBHI with a core and halo in neurons from the spinal cord of an FALS patient with a two-base pair deletion in the SOD1 gene. A Immunostaining for SOD1: immunoreactivity is mostly restricted to the halo. B Immunostaining for GPx1: immunoreactivity is located in the SOD1-positive portion of the LBHI. C Immunoreactivity for Prx2. Co-localization of the three proteins SOD1, GPx1 and Prx2 in the LBHI is evident. D–F Serial sections of a core and halo-type LBHI in a transgenic rat expressing human SOD1 with an H46R mutation. Immunostaining for SOD1 (D), GPx1 (E) and Prx2 (F). Similar stainability and immunolocalization of SOD1, GPx1 and Prx2 in the LBHI are observed (*LBHI* Lewy body-like hyaline inclusion, *FALS* familial amyotrophic lateral sclerosis, *SOD1* superoxide dismutase 1, *GPx1* glutathione peroxidase1, *Prx2* peroxiredoxin2). A–F No counterstaining. *Bars* A (also for B, C), D (also for E, F) 25 μm

A neuropil staining pattern similar to that for Prx2 was observed with GPx1; weak GPx1 immunoreactivity was diffusely seen in the neuropil in transverse sections of the

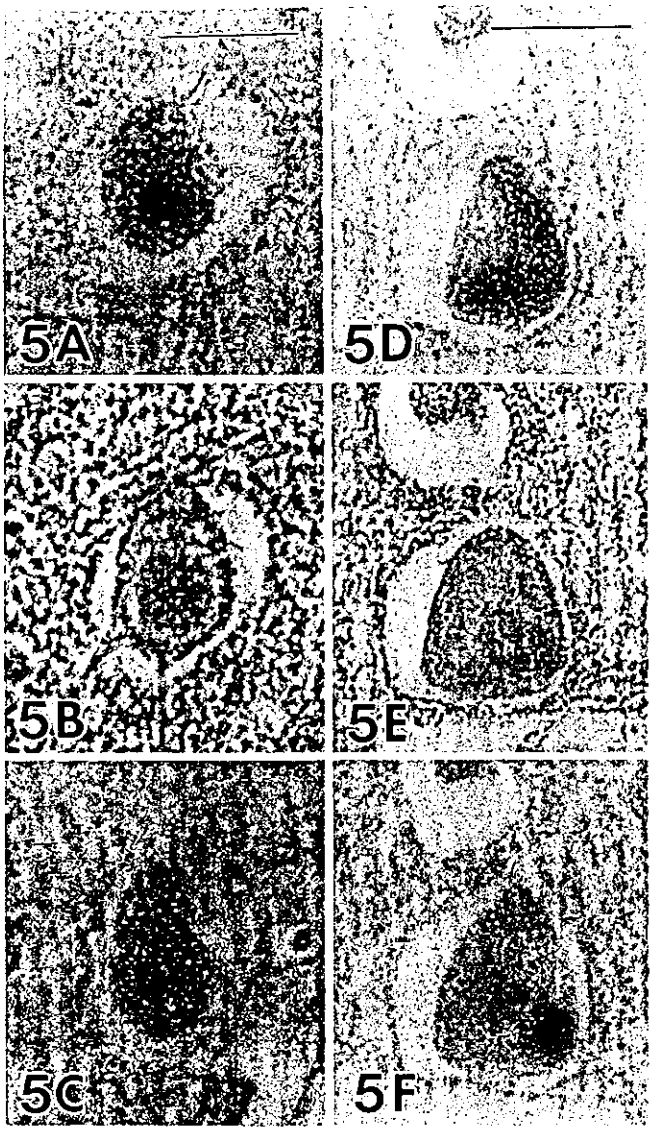

Fig. 5A–C Serial sections of an LBHI in an FALS patient with an A4V mutation in SOD1 gene. Immunostaining for SOD1 (A), GPx1 (B) and Prx2 (C). Co-localization of the three proteins in the LBHI is mainly observed in the core (A–C). D–F Serial sections of an LBHI in an FALS patient with a two-base pair deletion in the SOD1 gene. Immunostaining for SOD1 (D), GPx1 (E) and Prx2 (F). Immunostaining GPx1 (E) and Prx2 (F) are observed in only part of the SOD1-positive LBHI. The precise intra-inclusional immunolocalizations of these three proteins differ from each other in this LBHI (*LBHI* Lewy body-like hyaline inclusion, *FALS* familial amyotrophic lateral sclerosis, *SOD1* superoxide dismutase 1, *GPx1* glutathione peroxidase1, *Prx2* peroxiredoxin2). *Bars* A (also for B, C), D (also for E, F) 25 μm

spinal cords (Fig. 2A, B). GPx1 immunostaining was observed in the cytoplasm with cell bodies and proximal dendrites being essentially identified (Fig. 3A, B, E), but no intranuclear staining was observed (Fig. 3B, E). The stainability and intensity of Prx2 and GPx1 in the normal anterior horn cells of the spinal cords in humans were identical to those in rats. Therefore, almost all of the normal motor neurons in the spinal cords co-expressed both Prx2 and GPx1 (Fig. 3A–C), although the staining intensities of positively stained neurons varied.

Corroborating recent findings [12, 13, 16, 19, 27, 30], almost all of the neuronal LBHIs in both the FALS patients from two different families and races (Japanese Oki family and American C family) and the transgenic rats expressing two different human SOD1 mutations (H46R and G93A) were intensely immunostained by the antibody against human SOD1 (Figs. 4A, D; 5A, D; 6A; 7A). Most neuronal LBHIs were also immunoreactive for Prx2, although the intensity of Prx2 immunoreactivity in the LBHIs varied (Figs. 4C, F; 5C, F; 6B). The LBHIs in the neurons of the FALS patients and transgenic rats (H46R and G93A) showed a similar immunoreactivity for Prx2. The Prx2 immunolocalization in many intracytoplasmic and intraneuritic LBHIs was similar to that of SOD1 in both diseases. In core and halo-type LBHIs, the reaction product deposits of the antibody against Prx2 were generally restricted to the periphery (Fig. 4C, F), and were sometimes localized in the cores alone (Fig. 5C). In ill-defined LBHIs, Prx2 immunostaining was distributed throughout each inclusion. In some inclusions, however, expression of Prx2 was observed in only part of the inclusion (Fig. 5F). With respect to the GPx1 immunostaining in the neuronal LBHIs, similar stainability and immunolocalization to Prx2 were confirmed in the core and halo types as well as the ill-defined forms; most LBHIs in neurons were immunostained by the anti-GPx1 antibody with various intensities (Figs. 4B, E; 5B, E; 7B). The immunoreactivity for GPx1 in the FALS patients was similar to that in the transgenic rats (H46R and G93A). Like Prx2, the immunolocalization of GPx1 was similar to that of SOD1 in both diseases. GPx1-immunoreactive products in many core and halo-type inclusions were mainly localized in the periphery portions (Fig. 4B, E), but sometimes in the core portions alone (Fig. 5B). In some inclusions, the reaction products were confined to certain regions of each inclusion (Fig. 5E).

Noticeably, the co-localization of the three proteins SOD1, Prx2 and GPx1 in neuronal LBHIs in SOD1-mutated FALS patients and transgenic rats (H46R and G93A) was evident (Figs. 4, 5, 6, 7), although all three immunoreactive intensities varied. With respect to the intra-inclusional localization, many inclusions showed similar co-localizations of these three proteins (Figs. 4, 5A–C). In some LBHIs, the precise intra-inclusional immunolocalizations of the three proteins differed: Prx2 (Fig. 5D, F) and GPx1 (Fig. 5D, E) immunostaining was observed in only some areas of the SOD1-positive LBHIs.

Discussion

Under normal physiological conditions, Prx2 and GPx1 immunoreactivities in the spinal cord anterior horns in humans and rats are primarily identified in the neurons: cytoplasmic staining with both antibodies is observed in almost all of the anterior horn cells. Like Prx1 [26, 33], intranuclear localization in some neurons is also observed in Prx2 immunostaining. Considering that endogenous Prx2

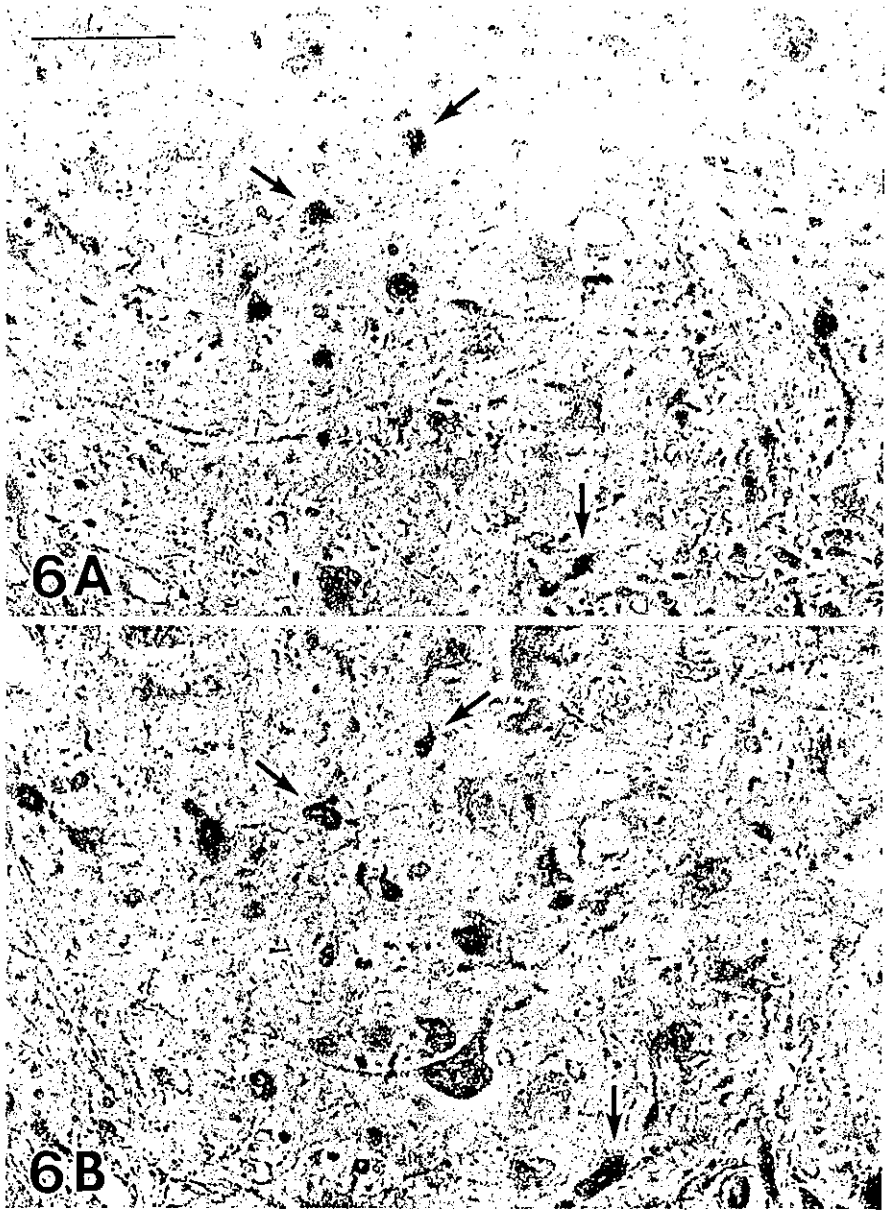

Fig. 6 Serial sections of the spinal anterior horn in a transgenic rat expressing human SOD1 with an H46R mutation immunostained with antibodies against SOD1 (**A**) and Prx2 (**B**). Round and sausage-like LBHIs in the neuropil are positive for both SOD1 and Prx2 (*arrows*) (*SOD1* superoxide dismutase1, *LBHI* Lewy body-like hyaline inclusion, *Prx2* peroxiredoxin2). *Bar* **A** (also for **B**) 50 μm

and GPx1 within the neuronal cytoplasm are extremely effective regulators of the redox system, our immunohistochemical finding that almost all of the normal spinal motor neurons co-expressed both Prx2 and GPx1 confirms that these motor neurons maintain themselves using the intracellular Prx2/GPx1 system, that is, the redox system.

As expected [12, 13, 16, 27, 30], SOD1 protein (probably the mutant form) was found to aggregate in the anterior horn cells as neuronal LBHIs in FALS patients with SOD1 gene mutations and transgenic rats expressing human SOD1 with H46R and G93A mutations. Intense co-expression of SOD1, Prx2, and GPx1 in neuronal LBHIs in both diseases was evident. To eliminate ROSs, SOD1-mutated motor neurons in mutant SOD1-linked FALS and transgenic rats (G46R and G93A) induce mutant/wild-type SOD1 as an antioxidant system and Prx2/GPx1 as a redox system. In this in vivo milieu where mutant SOD1 exists, Prx2 and GPx1 would aberrantly interact with the mutant SOD1, which is assumed to aggregate easily by itself [8]. Among the multiple theories of how mutant SOD1 contributes to motor neuron death in mutant SOD1-related FALS and transgenic animal models expressing human mutant SOD1, the aggregation of mutant SOD1 in neurons leads to part of the mutant SOD1-mediated toxicity through the formation of advanced glycation endproduct-modified SOD1 that is insoluble and cytotoxic [16]. Our recent study of FALS patients with a two-base pair deletion at codon 126 of the SOD1 gene (Oki family) and G85R transgenic mice has revealed that not only does mutant SOD1 provoke inclusion formation, but that normal SOD1 also co-aggregates in these inclusions [3]. Together with the facts that there are neuronal LBHIs positive for

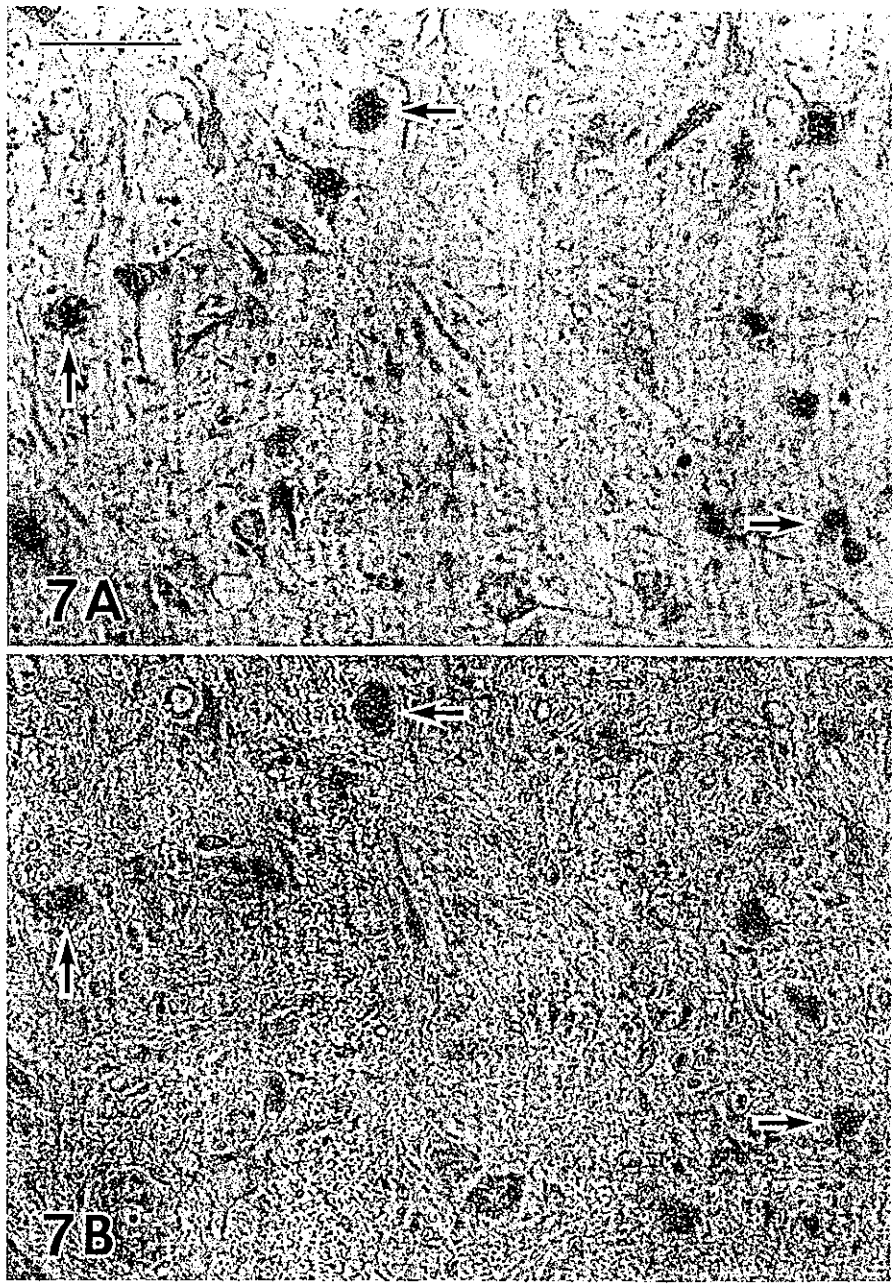

Fig. 7 Serial sections of the spinal anterior horn in a transgenic rat expressing human SOD1 with an H46R mutation immunostained with antibodies against SOD1 (A) and GPx1 (B). Round LBHIs in the neuropil are positive for both SOD1 and GPx1 (*arrows*) (*SOD1* superoxide dismutase1, *LBHI* Lewy body-like hyaline inclusion, *GPx1* glutathione peroxidase1). *Bar* A (also for B) 50 μm

SOD1, Prx2, and GPx1 in the milieu where mutant SOD1 exists but no LBHIs (no aggregations) exist under physiological conditions, our study demonstrates an aberrant interaction of Prx2/GPx1 with mutant SOD1, the aggregation of which results in neuronal LBHIs. In addition, intra-inclusional co-aggregation of Prx2/GPx1 with mutant SOD1 causes the intracytoplasmic reduction of Prx2/GPx1, thereby reducing the availability of the redox system. A similar aberrant interaction of the copper chaperone for SOD (CCS) and SOD1 (probably CCS-mutant SOD1) also occurs in the formation of the neuronal LBHIs in mutant SOD1-linked FALS [19] and the mutant SOD1 transgenic mouse model [32]. Such sequestration into LBHIs has also been observed for normal cytosolic constitutive proteins including tubulin and tau protein, as well as neuron-specific constitutive proteins containing phosphorylated neurofilament proteins (NFP), nonphosphorylated NFP, synaptophysin, and neuron-specific enolase [13, 17, 18]; this results in partial impairment of the maintenance of cell metabolism [13, 17, 18]. Although we cannot readily compare the sequestration of normal constitutive proteins with the aberrant interaction of cytotoxic mutant SOD1 with Prx2/GPx1 directly regulating a redox system, our finding leads us to speculate that not only co-aggregation of Prx2/GPx1 and SOD1 into LBHIs, but also intracytoplasmic reduction of Prx2/GPx1 in both diseases may partly contribute to the breakdown of the redox system itself in these SOD1-mutated neurons, and this may be one of the

endogenous mechanisms that accelerate neuronal death. This hypothesis would appear to be compatible with the aggregation toxicity theory. It remains to be determined whether this aberrant interaction of Prx2/GPx1 with mutant SOD1 is a direct or an indirect effect based on the pathogenesis of SOD1-mutated FALS disease itself or whether Prx2 and GPx1 play a primary or a secondary role to mutant SOD1. Consequently, we would like to emphasize that the aberrant interaction and co-aggregation of Prx2/GPx1 and SOD1 (probably Prx2/GPx1 and mutant SOD1) in FALS patients with SOD1 gene mutations and transgenic rats expressing human SOD1 mutations may amplify a more marked mutant SOD1-mediated toxicity.

Acknowledgements This study was supported in part by a Grant-in-Aid for Scientific Research (c) (2) from the Ministry of Education, Culture, Sports, Science and Technology of Japan (S.K.: 13680821) and by a Grant from the Ministry of Health, Labour and Welfare of Japan (S.K. and Y.I.).

References

1. Asayama K, Burr IM (1984) Joint purification of mangano and cuprozinc superoxide dismutases from a single source: a simplified method. Anal Biochem 136:336–339
2. Asayama K, Yokota S, Dobashi K, Hayashibe H, Kawaoi A, Nakazawa S (1994) Purification and immunoelectron microscopic localization of cellular glutathion peroxidase in rat hepatocytes: quantitative analysis by postembedding method. Histochemistry 102:213–219
3. Bruijn LI, Houseweart MK, Kato S, Anderson KL, Anderson SD, Ohama E, Reaume AG, Scott RW, Cleveland DW (1998) Aggregation and motor neuron toxicity of an ALS-linked SOD1 mutant independent from wild-type SOD1. Science 281: 1851–1854
4. Chae HZ, Kim IH, Kim K, Rhee SG (1993) Cloning, sequencing, and mutation of thiol-specific antioxidant gene of *Saccharomyces cerevisiae*. J Biol Chem 268:16815–16821
5. Chae HZ, Chung SJ, Rhee SG (1994) Thioredoxin-dependent peroxide reductase from yeast. J Biol Chem 269:27670–27678
6. Chae HZ, Robison K, Poole LB, Church G, Storz G, Rhee SG (1994) Cloning and sequencing of thiol-specific antioxidant from mammalian brain: alkyl hydroperoxide reductase and thiol-specific antioxidant define a large family of antioxidant enzymes. Proc Natl Acad Sci USA 91:7017–7021
7. De Haan JB, Bladier C, Griffiths P, Kelner M, O'Shea RD, Cheung NS, Bronson RT, Silvestro MJ, Wild S, Zheng SS, Beart PM, Hertzog PJ, Kola I (1998) Mice with a homozygous null mutation for the most abundant glutathione peroxidase, Gpx1, show increased susceptibility to the oxidative stress-inducing agents paraquat and hydrogen peroxide. J Biol Chem 273:22528–22536
8. Durham HD, Roy J, Dong L, Figlewicz DA (1997) Aggregation of mutant Cu/Zn superoxide dismutase proteins in a culture model of ALS. J Neuropathol Exp Neurol 56:523–530
9. Fridovich I (1986) Superoxide dismutases. Adv Enzymol Relat Area Mol Biol 58:61–97
10. Jin D-Y, Chae HZ, Rhee SG, Jeang K-T (1997) Regulatory role for a novel human thioredoxin peroxidase in NF-kappaB activation. J Biol Chem 272:30952–30961
11. Kato S, Shimoda M, Morita T, Watanabe Y, Nakashima K, Takahashi K, Ohama E (1996) Neuropathology of familial ALS with a mutation of the superoxide dismutase 1 gene. In: Nakano I, Hirano A (eds) Amyotrophic lateral sclerosis: progress and perspectives in basic research and clinical application. Elsevier Science, Amsterdam, pp 117–122
12. Kato S, Shimoda M, Watanabe Y, Nakashima K, Takahashi K, Ohama E (1996) Familial amyotrophic lateral sclerosis with a two base pair deletion in superoxide dismutase 1 gene: multisystem degeneration with intracytoplasmic hyaline inclusions in astrocytes. J Neuropathol Exp Neurol 55:1089–1101
13. Kato S, Hayashi H, Nakashima K, Nanba E, Kato M, Hirano A, Nakano I, Asayama K, Ohama E (1997) Pathological characterization of astrocytic hyaline inclusions in familial amyotrophic lateral sclerosis. Am J Pathol 151:611–620
14. Kato S, Horiuchi S, Nakashima K, Hirano A, Shibata N, Nakano I, Saito M, Kato M, Asayama K, Ohama E (1999) Astrocytic hyaline inclusions contain advanced glycation endproducts in familial amyotrophic lateral sclerosis with superoxide dismutase 1 gene mutation: immunohistochemical and immunoelectron microscopical analyses. Acta Neuropathol 97: 260–266
15. Kato S, Saito M, Hirano A, Ohama E (1999) Recent advances in research on neuropathological aspects of familial amyotrophic lateral sclerosis with superoxide dismutase 1 gene mutations: neuronal Lewy body-like hyaline inclusions and astrocytic hyaline inclusions. Histol Histopathol 14:973–989
16. Kato S, Horiuchi S, Liu J, Cleveland DW, Shibata N, Nakashima K, Nagai R, Hirano A, Takikawa M, Kato M, Nakano I, Ohama E (2000) Advanced glycation endproduct-modified superoxide dismutase-1 (SOD1)-positive inclusions are common to familial amyotrophic lateral sclerosis patients with SOD1 gene mutations and transgenic mice expressing human SOD1 with G85R mutation. Acta Neuropathol 100:490–505
17. Kato S, Takikawa M, Nakashima K, Hirano A, Cleveland DW, Kusaka H, Shibata N, Kato M, Nakano I, Ohama E (2000) New consensus research on neuropathological aspects of familial amyotrophic lateral sclerosis with superoxide dismutase 1 (SOD1) gene mutations: inclusions containing SOD1 in neurons and astrocytes. Amyotroph Lateral Scler Other Motor Neuron Disord 1:163–184
18. Kato S, Nakashima K, Horiuchi S, Nagai R, Cleveland DW, Liu J, Hirano A, Takikawa M, Kato M, Nakano I, Sakoda S, Asayama K, Ohama E (2001) Formation of advanced glycation end-product-modified superoxide dismutase-1 (SOD1) is one of the mechanisms responsible for inclusions common to familial amyotrophic lateral sclerosis patients with SOD1 gene mutation, and transgenic mice expressing human SOD1 gene mutation. Neuropathology 21:67–81
19. Kato S, Sumi-Akamaru H, Fujimura H, Sakoda S, Kato M, Hirano A, Takikawa M, Ohama E (2001) Copper chaperone for superoxide dismutase co-aggregates with superoxide dismutase 1 (SOD1) in neuronal Lewy body-like hyaline inclusions: an immunohistochemical study on familial amyotrophic lateral sclerosis with SOD1 gene mutation. Acta Neuropathol 102:233–238
20. Kato T, Hirano A, Kurland LT (1987) Asymmetric involvement of the spinal cord involving both large and small anterior horn cells in a case of familial amyotrophic lateral sclerosis. Clin Neuropathol 6:67–70
21. Kosower NS, Kosower EM (1978) The glutathione status of cells. Int Rev Cytol 54:109–160
22. Kurland LT, Mulder DW (1955) Epidemiologic investigations of amyotrophic lateral sclerosis. II. Familial aggregations indicative of dominant inheritance. Neurology 5:249–268
23. Matsumoto A, Okado A, Fujii T, Fujii J, Egashira M, Niikawa N, Taniguchi N (1999) Cloning of the peroxiredoxin gene family in rats and characterization of the fourth member. FEBS Lett 443:246–250
24. Meister A, Anderson ME (1983) Glutathione. Annu Rev Biochem 52:711–760
25. Mills GC (1957) Hemoglobin catabolism. 1. Glutathione peroxidase, an erythrocyte enzyme which protects hemoglobin from oxidative breakdown. J Biol Chem 229:189–197
26. Mu ZM, Yin XY, Prochownik EV (2002) Pag, a putative tumor suppressor, interacts with the Myc Box II domain of c-Myc and selectively alters its biological function and target gene expression. J Biol Chem 277:43175–43184

27. Nagai M, Aoki M, Miyoshi I, Kato M, Pasinelli P, Kasai N, Brown RH Jr, Itoyama Y (2001) Rats expressing human cytosolic copper-zinc superoxide dismutase transgenes with amyotrophic lateral sclerosis: associated mutations develop motor neuron disease. J Neurosci 21:9246–9254
28. Nakano I, Hirano A, Kurland LT, Mulder DW, Holley PW, Saccomanno G (1984) Familial amyotrophic lateral sclerosis. Neuropathology of two brothers in American "C" family. Neurol Med (Tokyo) 20:458–471
29. Sen CK, Packer L (1996) Antioxidant and redox regulation of gene transcription. FASEB J 10:709–720
30. Shibata N, Hirano A, Kobayashi M, Siddique T, Deng HX, Hung WY, Kato T, Asayama K (1996) Intense superoxide dismutase-1 immunoreactivity in intracytoplasmic hyaline inclusions of familial amyotrophic lateral sclerosis with posterior column involvement. J Neuropathol Exp Neurol 55:481–490
31. Takahashi K, Nakamura H, Okada E (1972) Hereditary amyotrophic lateral sclerosis. Histochemical and electron microscopic study of hyaline inclusions in motor neurons. Arch Neurol 27:292–299
32. Watanabe M, Dykes-Hoberg M, Culotta VC, Price DL, Wong PC, Rothstein JD (2001) Histological evidence of protein aggregation in mutant SOD1 transgenic mice and in amyotrophic lateral sclerosis neural tissues. Neurobiol Dis 8:933–941
33. Wen ST, Van Etten RA (1997) The PAG gene product, a stress-induced protein with antioxidant properties, is an Abl SH3-binding protein and a physiological inhibitor of c-Abl tyrosine kinase activity. Genes Dev 11:2456–2467

ACADEMIC PRESS

Available online at www.sciencedirect.com

SCIENCE DIRECT®

Biochemical and Biophysical Research Communications 303 (2003) 496–503

BBRC

www.elsevier.com/locate/ybbrc

Mutant SOD1 linked to familial amyotrophic lateral sclerosis, but not wild-type SOD1, induces ER stress in COS7 cells and transgenic mice☆

Shinsuke Tobisawa,[a,b] Yasukazu Hozumi,[b] Shigeki Arawaka,[a] Shingo Koyama,[a] Manabu Wada,[a] Makiko Nagai,[c] Masashi Aoki,[c] Yasuto Itoyama,[c] Kaoru Goto,[b] and Takeo Kato[a,*]

[a] *Third Department of Internal Medicine, Yamagata University School of Medicine, 2-2-2 Iida-Nishi, Yamagata 990-9585, Japan*
[b] *Department of Anatomy and Cell Biology, Yamagata University School of Medicine, Yamagata, Japan*
[c] *Department of Neurology, Tohoku University School of Medicine, Seidai, Japan*

Received 21 February 2003

Abstract

Mutations in a Cu, Zn-superoxide dismutase (SOD1) cause motor neuron death in human familial amyotrophic lateral sclerosis (FALS) and its mouse model, suggesting that mutant SOD1 has a toxic effect on motor neurons. However, the question of how the toxic function is gained has not been answered. Here, we report that the mutant SOD1s linked to FALS, but not wild-type SOD1, aggregated in association with the endoplasmic reticulum (ER) and induced ER stress in the cDNA-transfected COS7 cells. These cells showed an aberrant intracellular localization of mitochondria and microtubules, which might lead to a functional disturbance of the cells. Motor neurons of the spinal cord in transgenic mice with a FALS-linked mutant SOD1 also showed a marked increase of GRP78/BiP, an ER-resident chaperone, just before the onset of motor symptoms. These data suggest that ER stress is involved in the pathogenesis of FALS with an SOD1 mutation.

Keywords: Superoxide dismutase 1; Amyotrophic lateral sclerosis; Endoplasmic reticulum

Amyotrophic lateral sclerosis (ALS) is a neurodegenerative disease characterized by a selective loss of motor neurons in the motor cortex, brainstem, and spinal cord. Patients with ALS show progressive muscle weakness, atrophy, and, ultimately, death due to respiratory failure, which usually occurs within 3–5 years of the onset of the disease. In most cases, ALS occurs sporadically; however, there is a family history of the disease in 5–10% of the cases (familial ALS: FALS). It is known that approximately 20% of FALS is caused by a missense mutation of the Cu, Zn-superoxide dismutase (SOD1) gene [1,2]. FALS with an SOD1 mutation shows an adult-onset, autosomal dominant form of ALS. Until now, FALS-linked SOD1 mutations have been reported to occur at about 60 sites of the amino acid sequence of SOD1 (http://www.alsod.org) [3]. At first, a diminished superoxide scavenging activity of SOD1 mutant and subsequent oxidative stress were considered to be a pathogenic mechanism of FALS with an SOD1 mutation [1,2,4–6]. However, elimination of SOD1 in a knock-out mouse model did not cause any neurological symptoms or pathology [7]. Moreover, transgenic mice with a FALS-linked mutated SOD1 gene developed motor neuron symptoms and pathology irrespective of the degree of enzymatic activity of SOD1 [8–11]. In FALS patients, the age at the onset and the severity of the disease have no relationship to the degree of enzymatic activity of SOD1 [12–14]. Therefore, the functional loss

☆ *Abbreviations:* ALS, amyotrophic lateral sclerosis; ER, endoplasmic reticulum; FALS, familial amyotrophic lateral sclerosis; PBS, phosphate-buffered saline; SOD1, superoxide dismutase 1.

* Corresponding author. Fax: +81-23-628-5318.
E-mail address: tkato@med.id.yamagata-u.ac.jp (T. Kato).

0006-291X/03/$ - see front matter © 2003 Elsevier Science (USA). All rights reserved.
doi:10.1016/S0006-291X(03)00353-X

of SOD1 does not seem to be the pathogenesis of FALS with an SOD1 mutation [15]. Another hypothesis is a possible toxic function of the mutant SOD1, in which the mutant obtains an aberrant catalytic ability. This includes the peroxynitrate and the peroxidase hypotheses [16,17]. In the former, the mutation of SOD1 was speculated to disrupt the active-site pocket of the enzyme to allow the copper to react with peroxynitrite, resulting in the nitration of proteins [16]. In the latter, the FALS-associated mutant SOD1 has been shown in vitro to augment the catalytic oxidation of a model substrate by hydrogen peroxide [17]. However, these hypotheses are not supported by the observation that the elevation or elimination of wild-type SOD1 has no effect on the symptoms or pathology of a transgenic mouse model with FALS-linked mutant SOD1 [15].

It is known that misfolding of a protein after biosynthesis results in aggregation of the protein, which causes damage of cells including neurons [18–20]. In a transgenic mouse with mutated SOD1, formation of insoluble, high-molecular-weight complexes of mutated SOD1 was observed several months before the onset of the disease [21]. In this report, the FALS-linked mutant SOD1 transfected to COS7 cells induces endoplasmic reticulum (ER) stress by the accumulation of insoluble, mutant SOD1 and a possible dysfunction of the intracellular transport, which may explain how the mutant SOD1 causes the disease. Similar changes of the ER are also observed in transgenic mice with a mutant SOD1.

Experimental procedures

Plasmid constructs. Total RNA was extracted from human white blood cells by acid guanidinium thiocyanate–phenol–chloroform extraction. First-strand cDNA was prepared using the 1st-Strand cDNA Synthesis kit for RT-PCR (AMV) (Roche Molecular Biochemicals, Mannheim, Germany). A full-length wild-type SOD1 cDNA with *Eco*RI linker sequences was generated by polymerase chain reaction (PCR) using a primer pair of a sense primer (5′-CGGAATTCA TGGCGACGAAGGCCGTGTG-3′) and an anti-sense primer (5′-GG GAATTCTTATTGGGCGATCCCA-3′) followed by subcloning into the *Eco*RI-cleaved pcDNA3 with an epitope tag composed of eight amino acids (FLAG marker peptide, Asp–Tyr–Lys–Asp–Asp–Asp–Lys; Eastman Kodak) that was fused to wild-type SOD1 by cloning the 24 base pairs of the FLAG coding sequence upstream to the coding region of wild-type SOD1 cDNA. PCR amplification was performed by using Ex *Taq* DNA polymerase (Takara Shuzo Tokyo, Japan) according to the following schedule: 94 °C for 30 s, 60 °C for 30 s, and 72 °C for 90 s for 30 cycles. Mutant SOD1 cDNAs were generated by site-specific mutagenesis. Wild-type and mutant SOD1s were also subcloned with FLAG coding sequence into pEF-BOS, which utilizes the human polypeptide chain elongation factor 1α promoter (EF-1α) [22]. Rat diacylglycerol kinase ζ (DGK ζ) cDNA [23] was subcloned into pEGFP-C2 (Clontech, Palo Alto, CA, USA). These subcloned cDNAs were sequenced by the Model 310 Autosequencer (Applied Biosystems, Foster City, CA, USA).

Cell culture and transfection. COS7 cells were cultured in Dulbecco's modified Eagle's medium with 10% fetal bovine serum and transfected with 1 μg or co-transfected with 2 μg (1 μg each) of plasmid DNA using Lipofectamine 2000 (Invitrogen, Carlsbad, CA, USA) according to the manufacturer's instructions. Cultured cells were harvested 48 h after transfection and lysed by sonication in a lysis buffer containing 50 mM Tris–HCl (pH 7.6), 150 mM NaCl, 5 mM EDTA, 1 mg/L leupeptin, and 50,000 U/L trasylol. After removal of undisrupted cells by centrifugation (5000*g*, 7 min, 4 °C), the resultant supernatant was designated as the *total lysate*. Protein concentrations were determined by the bicinchoninate method. Cytosol fraction was prepared according to the following method: the supernatant resulting from the removal of nuclear fraction by centrifugation (14,000*g*, 10 min, 4 °C) was ultracentrifuged (100,000*g*, 1 h, 4 °C). The resultant supernatant was designated as the *cytosol fraction*. The *pellet* was resuspended in a lysis buffer that equaled the cytosol fraction in volume.

Immunoblotting. The total lysate from COS7 cells was prepared as described above. Ten micrograms of total protein boiled for 5 min in a 3 × SDS sample buffer (New England Biolabs, Beverly, MA, USA) was subjected to 15% SDS–polyacrylamide gel electrophoresis. The separated proteins were then electrophoretically transferred onto a PolyScreen-PVDF membrane (NEN TM Life Science Products, USA). After blocking non-specific binding sites in 5% skim milk (w/v) in phosphate-buffered saline (PBS) with 0.01% Tween 20, the membrane was incubated for 1 h at room temperature with the antibody against FLAG or GRP78/BiP and then treated with peroxidase-conjugated anti-mouse or anti-rabbit IgG antibodies for 1 h. The immunoreactive bands were detected using a chemi-luminescence detection kit (ECL Western blotting kit, Amersham, Uppsala, Sweden). The cytosol and pellet fractions were prepared as described above. Ten microliters each of both fractions and total lysate were subjected to immunoblotting and the immunoreactive bands were detected using the same methods as described above.

Immunocytochemistry of cDNA-transfected COS7 cells. After transfection and a 24-h incubation, cells were fixed in 4% paraformaldehyde in a 0.1 M sodium phosphate buffer (pH 7.2), followed by a 0.1% Triton X-100 permeabilization for 5 min. After fixation, cells were washed extensively in PBS and blocked with PBS containing 5% normal goat serum (NGS) for 15 min. The cells were incubated with the following appropriate primary antibodies diluted in PBS containing 5% NGS: mouse anti-FLAG (M2) antibody (1 μl/ml, Sigma-Aldrich, St. Louis, MO, USA), rabbit anti-GRP78/BiP antibodies (diluted 1:1000, Stressgen), rabbit anti-SOD2 antibodies (diluted 1:10,000, provided by Dr. K. Asayama, University of Occupational and Environmental Health, Japan), and rabbit anti-tubulin antibodies (diluted 1:10,000, provided by Dr. R. Kuwano, Niigata University, Japan) for 1 h at room temperature. Cells were washed for 5 × 5 min in PBS and incubated with the following appropriate secondary antibodies diluted in PBS containing 5% NGS: anti-mouse IgG conjugated to Alexa 546 (diluted 1:250, Molecular Probes, Eugene, OR, USA) and biotinylated anti-rabbit IgG (diluted 1:250, Vector Laboratories, Burlingame, CA, USA) for 30 min at room temperature. Cells incubated with biotinylated anti-rabbit IgG antibodies were washed 5 × 5 times in PBS and incubated with streptavidin conjugated to Alexa 488 (10 μg/ml) for 30 min at room temperature. Cells were counterstained with the following markers for organelle and cytoskeleton according to the manufacturer's instructions: ER-Tracker (endoplasmic reticulum; ER marker, Molecular Probes), BODIPY FL-C5 ceramide (Golgi marker, Molecular Probes), and Alexa Fluor TM 568 phalloidin (Actin marker, Molecular Probes). Transfected cells with SOD1s in pcDNA3 were incubated with or without 10 μM lactacystin for 24 h. Stained cells were observed using a laser scanning confocal microscope (LSM 5 PASCAL, Zeiss, Germany).

Immunohistochemistry of transgenic mice with mutated SOD1. Formalin-fixed, paraffin-embedded tissue sections of the spinal cord were used from two lines of transgenic mice with SOD1 mutations, L84V (M. Kato, et al. Transgenic mice with ALS-linked SOD1 mutant L84V. Abstract of the 31st Annual Meeting of Society for Neuroscience, San Diego, 2001) and H46R (M. Nagai, et al. Transgenic mice with ALS-linked SOD1 mutant H46R. Abstract of the 30th Annual Meeting of Society for Neuroscience, 2000) and age-matched

non-transgenic mice. Deparaffinized sections were incubated with 1% hydrogen peroxide for 15 min, followed by 10% normal goat serum. The sections were subsequently incubated with anti-GRP78/BiP antibodies (diluted 1:1000, Stressgen, Victoria, BC, Canada) at 4 °C for 48 h. Labeling was visualized by the method described previously [24].

Results

An epitope tag composed of eight amino acids (FLAG marker peptide, Asp–Tyr–Lys–Asp–Asp–Asp–Lys) was fused upstream to the coding region of the wild-type and mutated SOD1 cDNA. Each of the cDNAs of the wild-type SOD1 and four mutant SOD1s linked to FALS (G37R, G85R, G93A, and S134N) was subcloned into two different expression vectors, pcDNA3 and pEF-BOS, and transfected into COS7 cells. After transfection and a 48-h culture, the cells were processed for Western blot analysis and immunocytochemistry.

The expression of wild-type and four FALS-linked mutant SOD1s in COS7 cells was confirmed by Western blot anlaysis of lysates using the anti-FLAG (M2) monoclonal antibody (Fig. 1). The molecular size of G85R was smaller than those of wild-type and the other mutants (Figs. 1A and B). Both wild-type and mutant SOD1s were expressed at much higher levels using pEF-BOS than pcDNA3 (Figs. 1A and B). The expression level of wild-type SOD1 in pEF-BOS was about 8.8 times as high as that in pcDNA3, and the expression levels of mutant SOD1s in pEF-BOS were 2.0 to 8.3 times as high as those in pcDNA3 by densitometry. Using pEF-BOS, the expression levels of mutant SOD1s were about 16–49% of the wild-type SOD1 by densitometry (Fig. 1A). On the other hand, such a marked decrease in the expression of mutant SOD1s was not apparent when pcDNA3 was employed (Fig. 1B). Using pEF-BOS, although the wild-type SOD1 was almost completely recovered in the cytosol fraction, a small amount of the mutant SOD1 protein remained in the pellet (Fig. 1C). Mutant G93A SOD1 protein in the pellet was about 30% of the total protein by densitometry (Fig. 1D).

Using pcDNA3, wild-type and mutant SOD1s were expressed and distributed diffusely throughout the cytoplasm of the transfected COS7 cells (Fig. 2). There was no obvious difference in the distribution pattern among them. Using pEF-BOS, the wild-type SOD1 also located diffusely in the cytoplasm, a result similar to that with the use of pcDNA3 (Fig. 2). On the other hand, mutant SOD1 expression using pEF-BOS produced

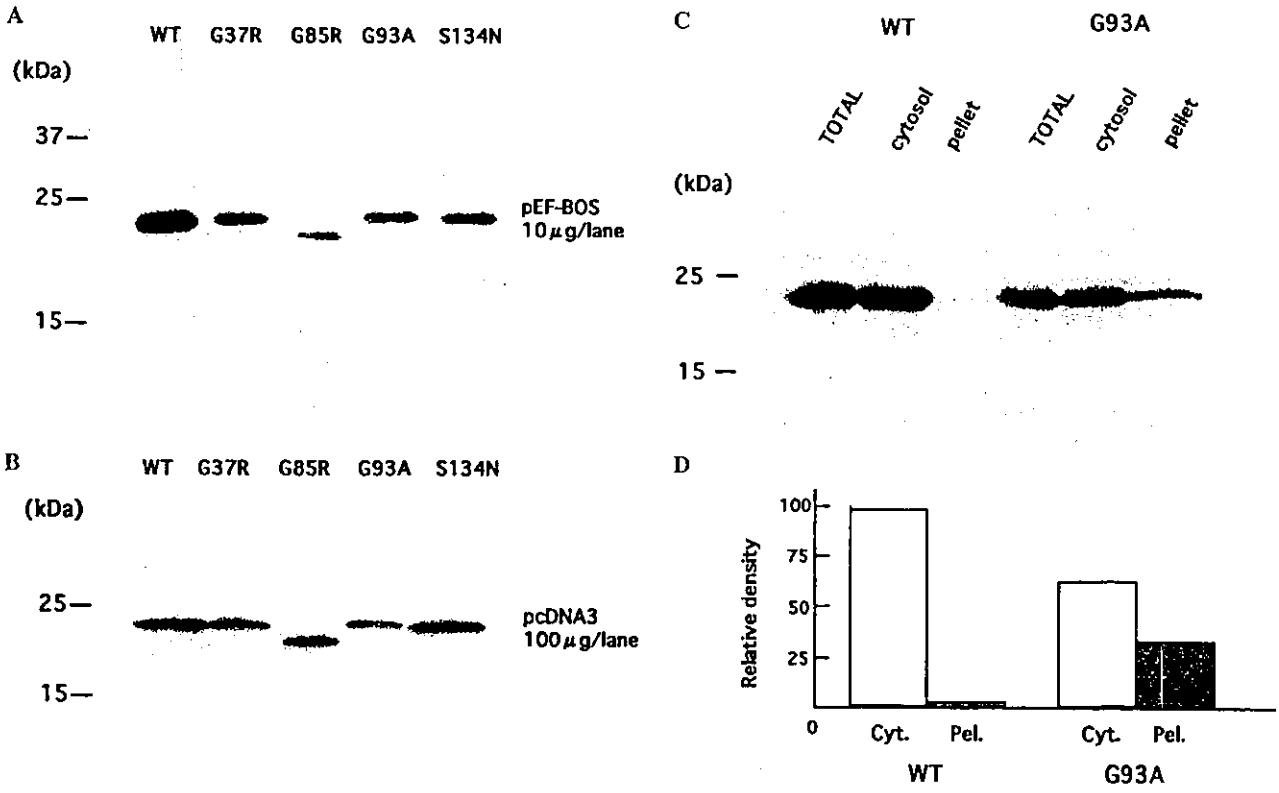

Fig. 1. Immunoblot analysis of wild-type (WT) and mutant (G37R, G85R, G93A, and S134N) SOD1s in total cell lysates derived from COS7 cells 48 h after transfection with SOD1 cDNA in pEF-BOS (A) or pcDNA3 (B). Ten mg (A) or 100 μg (B) of protein is applied to each lane. WT SOD1 expressed in COS7 cells is almost completely recovered in the cytosol fraction, whereas ~30% of mutant (G93A) SOD1 is in the pellet (C, D). Cyt, cytosol fraction; Pel, pellet. Expressed SOD1 is detected by anti-FLAG antibody (A–C). (D) Densitometry analysis (the density of wild-type SOD1 in cytosol fraction = 100%).

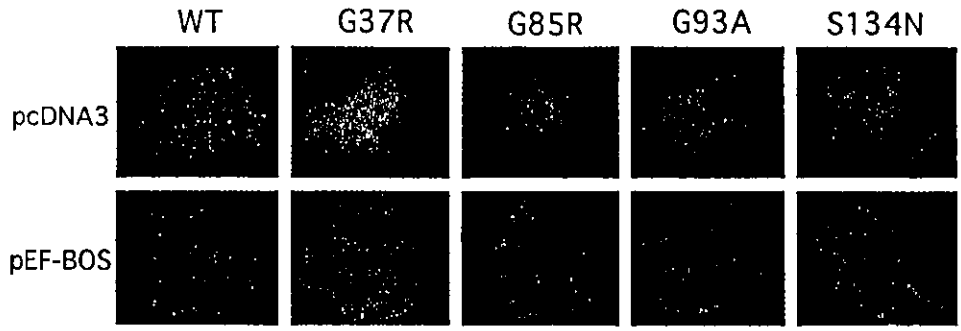

Fig. 2. Fluorescent microscopy of COS7 cells expressing wild-type (WT) and mutant (G37R, G85R, G93A, and S134N) SOD1s using pcDNA3 (upper panels) or pEF-BOS (lower panels). WT and mutant SOD1s expressed by pcDNA3 show a diffuse distribution in the cytoplasm. WT SOD1 expressed by pEF-BOS also shows a diffuse distribution, whereas mutant SOD1s by pEF-BOS produce an aggregate formation in the perinuclear area of the cytoplasm. Expressed SOD1 is detected by an anti-FLAG antibody.

aggregates of the mutant protein in the perinuclear region of the cytoplasm (Fig. 2). The cells containing these aggregates comprised 5–20% of the total transfected cells.

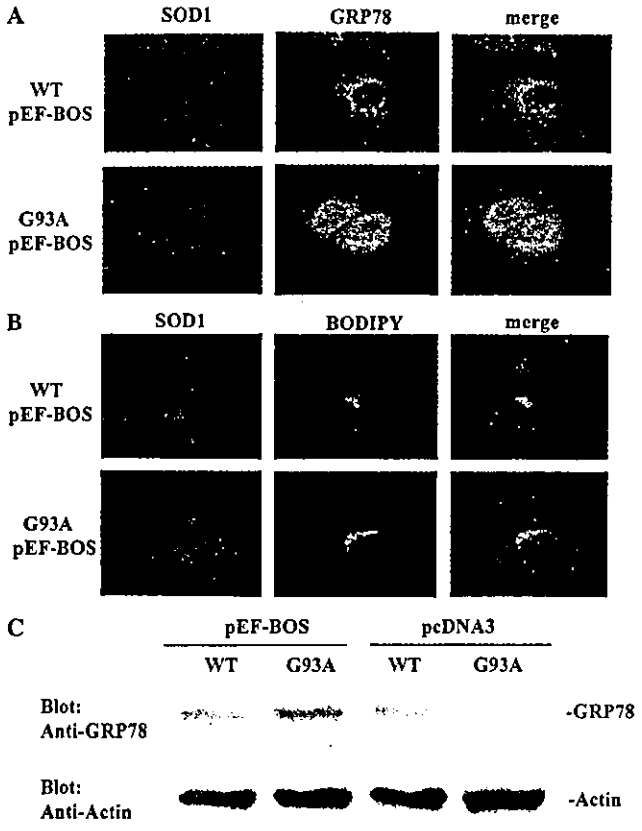

Fig. 3. COS7 cells expressing WT (upper panels) or mutant (G93A) SOD1 (lower panels) using pEF-BOS. (A) Double-staining with anti-FLAG (red) and anti-GRP78 (green) antibodies. Perinuclear aggregates of mutant SOD1 are colocalized with GRP78, an ER marker (lower panels). The overexpression of GRP78 is also observed in a mutant SOD1-expressing cell (middle in lower panels). (B) Double-labeling with anti-FLAG antibody (red) and BODIPY FL-C5 ceramide, a Golgi marker (green). (C) Immunoblot analysis showing that GRP78 expression is increased in COS7 cells transfected with a mutant (G93A) SOD1 cDNA in pEF-BOS.

The subcellular localization of the mutation-related perinuclear aggregates was then examined. COS7 cells expressing wild-type SOD1 or mutant SOD1s were double-stained with the anti-FLAG (M2) antibody and the ER markers (ER tracker and anti-GRP78/BiP antibody) or the Golgi marker (BODIPY-C5 ceramide) (Fig. 3). In the COS7 cells transfected with the wild-type SOD1 cDNA in pcDNA3 or pEF-BOS, both the ER (Fig. 3A) and Golgi apparatus (Fig. 3B) showed a normal morphology in the juxta-nuclear position. In the cells transfected with a mutant SOD1 cDNA in pEF-BOS, on the other hand, perinuclear aggregates of mutant SOD1 colocalized with the two ER markers (Fig. 3A), indicating accumulation of aggregated mutant SOD1 in or on the ER. A volume expansion of the ER in these cells was also observed. Western blot analysis confirmed an increase in the expression of GRP78/BiP in these cells (Fig. 3C). However, the aggregate of the mutant SOD1 was not colocalized with the Golgi marker (Fig. 3B), indicating that Golgi complex is not involved.

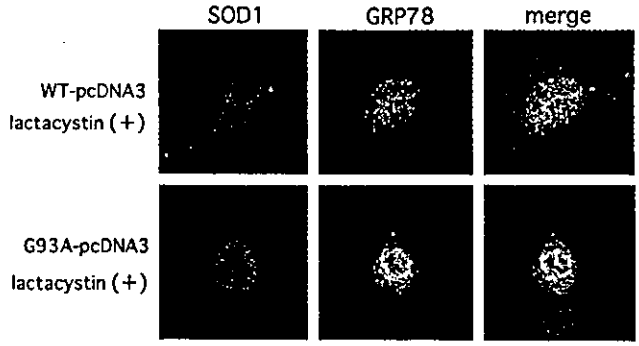

Fig. 4. COS7 cells expressing WT (upper panels) or mutant (G93A) SOD1 (lower panels) using pcDNA3 double-stained with anti-FLAG (red) and anti-GRP78 (green) antibodies. The exposure to lactacystin, a proteasome inhibitor, produces perinuclear aggregates of mutant SOD1, but not WT SOD1. Overexpression of GRP78 is also seen in a cell with aggregate formation of mutant SOD1 (middle in lower panels).

To examine the involvement of the proteasome function in the formation of perinuclear aggregates, a proteasome inhibitor, lactacystin, was used. When cells expressing wild-type or mutant SOD1s using pcDNA3 were exposed to 10 μM lactacystin for 24 h, perinuclear aggregates of SOD1 occurred in the cells expressing the mutant, but not the wild-type, SOD1 (Fig. 4). Perinuclear aggregates were colocalized with the ER markers and the ER was seen to be expanded (Fig. 4). These changes were almost identical to those of the mutant SOD1s expressed by pEF-BOS. This suggests that mutant SOD1s were degraded by proteasome and that the suppression of proteasome activity by lactacystin caused an accumulation of mutant SOD1 in association with the ER.

The influence of perinuclear aggregates of mutated SOD1 on the cytoskeleton and mitochondria was examined next. In the cells expressing wild-type SOD1 using pEF-BOS, actin stress fibers visualized by phalloidin-Alexa 568 were abundant in number and distributed to both the perinuclear and peripheral areas of the cytoplasm (Fig. 5A). In the cells expressing mutant SOD1s using pEF-BOS, actin stress fibers were obviously decreased in number, but their organization and distribution seemed unchanged (Fig. 5A). Microtubules detected by the anti-tubulin antibodies were observed to radiate to the periphery of the cytoplasm from the centrosome in the cells expressing wild-type SOD1 using pEF-BOS (Fig. 5B). In the cells expressing mutant SOD1s using pEF-BOS, however, the fiber formation of tubulin was disrupted and the location of tubulin was restricted to the perinuclear area of the cytoplasm (Fig. 5B). Mitochondria detected by the anti-SOD2 antibodies showed a normal morphology and distribution in the cytoplasm of cells expressing wild-type SOD1 using pEF-BOS (Fig. 5C). In cells expressing mutant SOD1 using pEF-BOS, however, mitochondria were confined to the perinuclear area of the cytoplasm and showed a

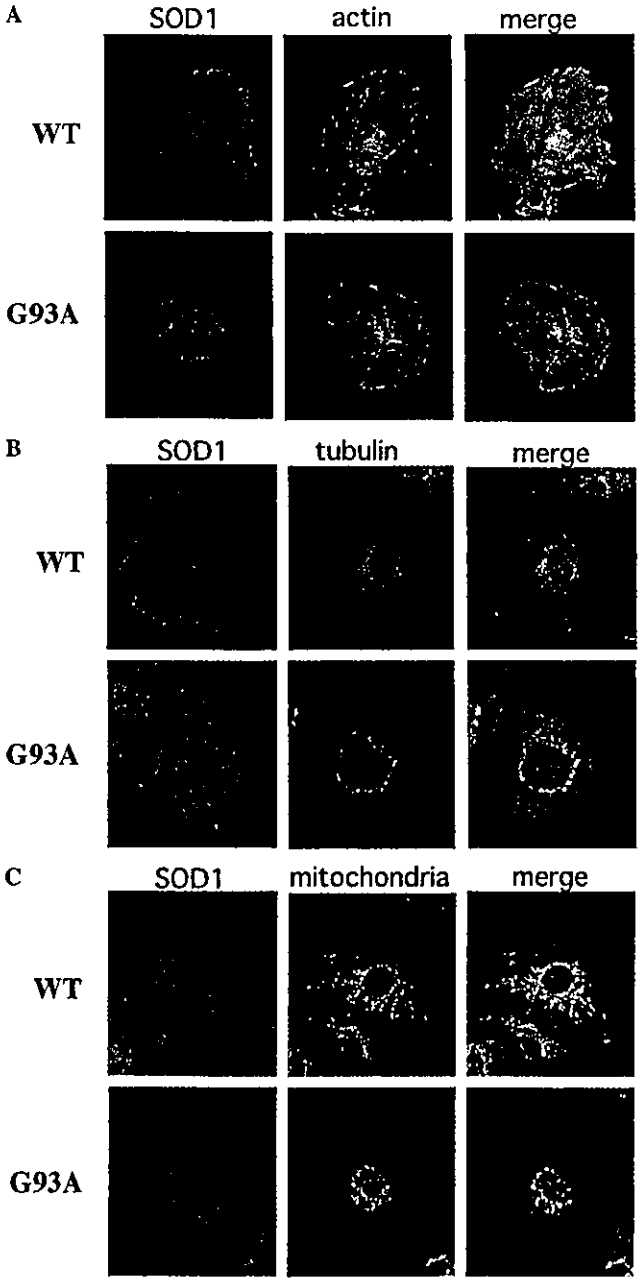

Fig. 5. COS7 cells expressing WT (upper panels) or mutant (G93A) SOD1 (lower panels) using pEF-BOS. (A) Double-staining with anti-FLAG antibody (red) and Alexa Fluor TM 568 phalloidin (green), an actin marker. Actin stress fibers are decreased in number, but their intracytoplasmic distribution seems unchanged in a cell with aggregate formation of mutant SOD1 (middle in lower panels). (B) Double-staining with anti-FLAG (red) and anti-tubulin (green) antibodies. Tubulin is restricted to the perinuclear area and does not show a fibrous appearance in a cell with aggregate formation of mutant SOD1 (middle in lower panels). (C) Double-staining with anti-FLAG (red) and anti-SOD2 (green) antibodies. SOD2, a marker of mitochondria, is restricted to the perinuclear area in a cell with aggregate formation of mutant SOD1 (middle in lower panels).

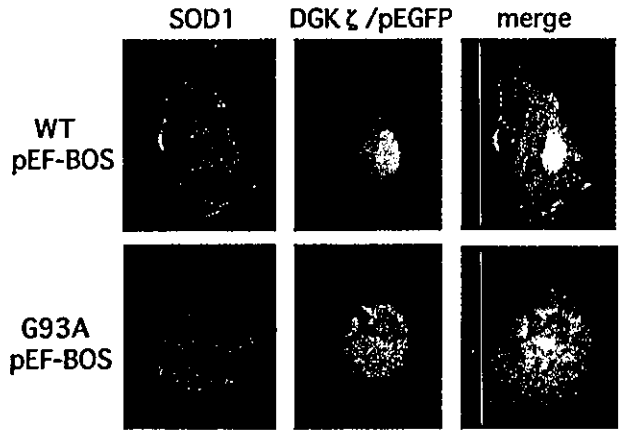

Fig. 6. COS7 cells co-transfected with WT (upper panels) or mutant (G93A) (lower panels) SOD1 (red) cDNA in pEF-BOS and diacylglycerol kinase ζ (DGK ζ) (green) cDNA in pEGFP-C2. Expressed DGK ζ, normally localized in the nucleus (middle in upper panels), does not reach the nucleus in a cell with aggregate formation of mutant SOD1 (middle in lower panels).

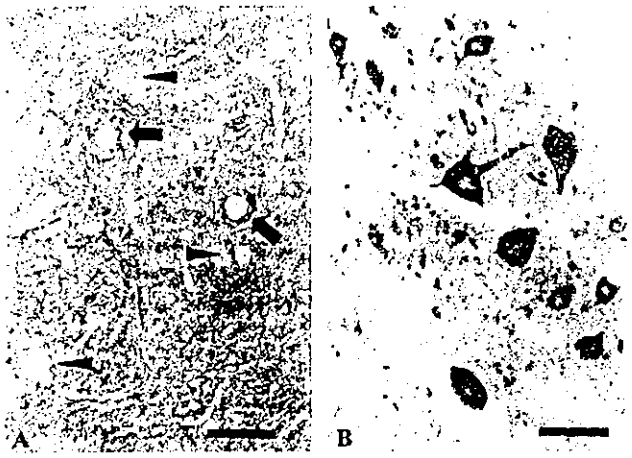

Fig. 7. Motor neurons of the spinal cord in non-transgenic (A) and transgenic mice with SOD1 mutation (L84V) (B), immunostained with anti-GRP78/BiP. Intense immunoreactivity is seen in virtually all motor neurons in a mouse with L84V mutation of the SOD1 transgene (B), although a few motor neurons (arrows) show a weak immunostaining in a non-transgenic mouse (A). The arrowheads indicate unstained motor neurons. Bar = 50 μm.

coarse appearance suggesting a morphology of mitochondrial swelling (Fig. 5C).

To examine the influence of aggregate formation on the localization of other proteins, a nuclear protein, diacylglycerol kinase ζ (DGK ζ) [23], was used. In co-transfected cells with wild-type SOD1 in pEF-BOS and rat DGK ζ in pEGFP, the expressed DGK ζ was localized in the nucleus (Fig. 6) as described previously [23]. In co-transfected cells with mutant SOD1s in pEF-BOS and DGK ζ in pEGFP, on the other hand, most DGK ζ remained in the cytoplasm and colocalized with the aggregates of mutant SOD1s, but did not reach the nucleus (Fig. 6).

For the investigation of ER changes in the mouse model of FALS, two lines of transgenic mice (L84V and H46R) and age-matched non-transgenic mice were used. These two transgenic mice showed an intense immunostaining of GRP78/BiP, an ER chaperone, in the cytoplasm of virtually all motor neurons of the spinal cord just before the onset of motor symptoms, whereas the non-transgenic mice showed a weak immunostaining in a few motor neurons (Fig. 7).

Discussion

The present study demonstrates that the FALS-linked mutation of SOD1 leads to aggregate formation in the cDNA-transfected COS7 cells in the condition that either drives gene expression at a high level (pEF-BOS) or suppresses the proteasome activity by lactacystin. The finding that FALS-linked mutant SOD1 was aggregated in transfected cultured cells has been reported by the previous studies [25,26]. Here we show for the first time that the pathological process is clearly dependent on the expression level of the mutants and the activity level of protein degradation. It should also be noted that the mutation-related aggregates are colocalized with the expanded ER. The results strongly suggest association of the aggregate with the ER.

The function of most proteins depends on the proper three-dimensional conformation of their mature, folded forms. Misfolding or unfolding of proteins after biosynthesis can be repaired through the quality-control system of the ER [27]. An accumulation of misfolded or unfolded proteins in the ER induces ER stress, in which three different mechanisms are known to be activated: transcriptional induction of ER-resident chaperones, translational attenuation of the misfolded or unfolded proteins, and their degradation through the ubiquitin-proteasome system [27]. In the present study, the decreased solubility of mutant SOD1 proteins in the cytosol (Fig. 1D) suggests a conformational change of the mutant proteins. This is in agreement with the report that insoluble, high-molecular-weight complexes of mutant SOD1 are detectable several months before the onset of the disease in a mouse model with a FALS-linked mutant SOD1 transgene [21]. Our observation revealed not only colocalization of the aggregated mutant proteins with the ER markers but also the up-regulation of GRP78/BiP expression in the transfected COS7 cells (transcriptional induction). In the high-expression system (pEF-BOS), on the other hand, the amount of mutant SOD1 proteins in the transfected COS7 cells was less than that in the wild-type SOD1, suggesting a translational attenuation or an increase in the degradation of the mutants. The inhibition of proteasome activity by lactacystin exposure produced an aggregation of mutant SOD1 in the lower-expression system (pcDNA3), indicating that the proteasome system is involved in the degradation of the mutant proteins. All these results are compatible with the quality-control system of the ER described above, demonstrating that the mutant SOD1s linked to FALS might induce ER stress in the transfected COS7 cells. In such cells, tubulin and mitochondria did not reach their proper intracellular locations, but were confined to the perinuclear region. The fluorescent images of tubulin and mitochondria were seen to be just surrounded by the aggregates (Figs. 5B and C), suggesting that outgrowth of tubulin from the centrosome was spatially blocked by the aggregates. The mitochondrial dislocation may be due to a restricted tubulin outgrowth, because this organelle is transported throughout the cytoplasm on microtubules, but not actin filament. A nuclear protein, DGK ζ, which was co-transfected with mutant SOD1 into COS7 cells, was also colocalized with the aggregates of the mutant associated with the ER. These data suggest that even non-mutated proteins suffer from ER dysfunction and are trapped in the

aggregates in an overexpression condition beyond a physiological condition. Considering that the very early change in transgenic mice with FALS-linked SOD1 mutation is an impairment of axonal transport [28], it seems that the FALS-linked mutant SOD1 also caused an impairment of the intracellular transport system in the transfected COS7 cells.

With regard to the subcellular localization of SOD1, the previous studies have reported that SOD1 is preferentially synthesized by free ribosomes in the in vitro experiments [29] and is localized mainly in the cytoplasm and the nucleus and partially in mitochondria [30–32]. In pathologic conditions such as hepatitis and cirrhosis, however, SOD1 has been shown to localize in the ER, vesicles, and Golgi complex in hepatocytes [33]. Little is known about the mechanism how SOD1 is transported from the cytoplasm to the membranous organelles, although it is reported that the mitochondrial accumulation of SOD1 is strongly influenced by the copper chaperone [34]. In the present study, although the aggregated mutant SOD1 was closely associated with the expanded ER, it remains unclear whether it is localized within the cistern of the ER or outside.

In human FALS with an SOD1 mutation, there are two major mysteries: motor neuron selectivity and adult onset. Although every cell has mutant SOD1 in FALS patients, the motor neurons seem to degenerate selectively. The answer to this mystery is that the functional integrity of motor neurons is critically dependent on vigorous intracellular transport, especially axonal transport, because a motor neuron has an enormously long axon (about 1 m in length). The dysfunction of intracellular transport, the degree of which does not have an apparent effect on the function or survival of non-motor neurons or non-nerve cells, may do great damage to motor neurons. The other mystery is the adult onset of the disease in spite of the presence of mutant SOD1 even in newborns. In the present study, a lower expression of the mutant SOD1 by the pcDNA3 vector did not produce any aggregation of the mutant protein or induce ER stress. However, the inhibition of proteasome activity by exposure to lactacystin produced an aggregation of the mutant protein and a dislocation of tubulin, mitochondria, and DGK ζ. The proteasome activity has been reported to decrease with aging in animals [35]. A decrease in proteasome activity paired with aging may allow the insoluble, high-molecular-weight complexes of mutant SOD1 to be accumulated beyond a non-compensable level in both patients and transgenic mice with a FALS-linked SOD1 mutation, resulting in the adult onset of the disease.

It has been shown that the knock-out of the SOD1 gene does not produce any neurological symptoms or pathologic changes in mice [7] and that the overexpression of wild-type SOD1 does not modulate the pathology in transgenic mice with the FALS-linked mutant SOD1 [15]. Thus, a decrease or increase in SOD1 activity, as well as the formation of peroxynitrite and subsequent tyrosine nitration of proteins, seems to be unrelated to the pathogenesis of FALS with an SOD1 mutation. Recently, a conformational change of a certain protein and subsequent ER stress have been shown to be an important step in the pathogenesis of neurodegenerative diseases, such as Alzheimer's disease, Parkinson's disease, and Creutzfeldt-Jakob disease [18–20,36,37]. The present study demonstrates that the FALS-linked mutant SOD1 caused ER stress and a possible disruption of the intracellular transport in the transfected COS7 cells, which may explain how the mutant SOD1 gains a toxic function. In transgenic mice with SOD1 mutation, the overexpression of GRP78/BiP, an ER-resident chaperone, was also observed in motor neurons of the spinal cord before onset of the disease. These data suggest that ER stress is involved in the pathogenesis of FALS with an SOD1 mutation. It seems that human FALS with an SOD1 mutation is also a conformational disease of the SOD1 molecule.

Acknowledgments

We are grateful to Professor Kimishige Ishizaka, La Jolla Institute for Allergy & Immunology, for critically reviewing the manuscript. This work was supported by grants from the Ministry of Education, Science, Sports and Culture of Japan, and from the Ministry of Health and Welfare of Japan.

References

[1] D.R. Rosen, Mutations in Cu/Zn superoxide dismutase gene are associated with familial amyotrophic lateral sclerosis, Nature 364 (1993) 362.
[2] H.X. Deng, A. Hentati, J.A. Tainer, Z. Iqbal, A. Cayabyab, W.Y. Hung, E.D. Getzoff, P. Hu, B. Herzfeldt, R.P. Roos, Amyotrophic lateral sclerosis and structural defects in Cu, Zn-superoxide dismutase, Science 261 (1993) 1047–1051.
[3] C.E. Shaw, Z.E. Enayat, B.A. Chioza, A. Al Chalabi, A. Radunovic, J.F. Powell, P.N. Leigh, Mutations in all five exons of SOD-1 may cause ALS, Ann. Neurol. 43 (1998) 390–394.
[4] M. Aoki, M. Ogasawara, Y. Matsubara, K. Narisawa, S. Nakamura, Y. Itoyama, K. Abe, Mild ALS in Japan associated with novel SOD mutation, Nat. Genet. 5 (1993) 323–324.
[5] R. Orrell, J. de Belleroche, S. Marklund, F. Bowe, R. Hallewell, A novel SOD mutant and ALS, Nature 374 (1995) 504–505.
[6] A.C. Bowling, J.B. Schulz, R.H. Brown Jr., M.F. Beal, Superoxide dismutase activity, oxidative damage, and mitochondrial energy metabolism in familial and sporadic amyotrophic lateral sclerosis, J. Neurochem. 61 (1993) 2322–2325.
[7] A.G. Reaume, J.L. Elliott, E.K. Hoffman, N.W. Kowall, R.J. Ferrante, D.F. Siwek, H.M. Wilcox, D.G. Flood, M.F. Beal, R.H. Brown Jr., R.W. Scott, W.D. Snider, Motor neurons in Cu/Zn superoxide dismutase-deficient mice develop normally but exhibit enhanced cell death after axonal injury, Nat. Genet. 13 (1996) 43–47.
[8] M.E. Gurney, H. Pu, A.Y. Chiu, M.C. Dal Canto, C.Y. Polchow, D.D. Alexander, J. Caliendo, A. Hentati, Y.W. Kwon, H.X.

Deng, Motor neuron degeneration in mice that express a human Cu, Zn- superoxide dismutase mutation, Science 264 (1994) 1772–1775.
[9] P.C. Wong, C.A. Pardo, D.R. Borchelt, M.K. Lee, N.G. Copeland, N.A. Jenkins, S.S. Sisodia, D.W. Cleveland, D.L. Price, An adverse property of a familial ALS-linked SOD1 mutation causes motor neuron disease characterized by vacuolar degeneration of mitochondria, Neuron 14 (1995) 1105–1116.
[10] M.E. Ripps, G.W. Huntley, P.R. Hof, J.H. Morrison, J.W. Gordon, Transgenic mice expressing an altered murine superoxide dismutase gene provide an animal model of amyotrophic lateral sclerosis, Proc. Natl. Acad. Sci. USA 92 (1995) 689–693.
[11] L.I. Bruijn, M.W. Becher, M.K. Lee, K.L. Anderson, N.A. Jenkins, N.G. Copeland, S.S. Sisodia, J.D. Rothstein, D.R. Borchelt, D.L. Price, D.W. Cleveland, ALS-linked SOD1 mutant G85R mediates damage to astrocytes and promotes rapidly progressive disease with SOD1-containing inclusions, Neuron 18 (1997) 327–338.
[12] T. Siddique, D. Nijhawan, A. Hentati, Molecular genetic basis of familial ALS, Neurology 47 (1996) S27–S34.
[13] D.R. Borchelt, M.K. Lee, H.S. Slunt, M. Guarnieri, Z.S. Xu, P.C. Wong, R.H. Brown Jr., D.L. Price, S.S. Sisodia, D.W. Cleveland, Superoxide dismutase 1 with mutations linked to familial amyotrophic lateral sclerosis possesses significant activity, Proc. Natl. Acad. Sci. USA 91 (1994) 8292–8296.
[14] D.W. Cleveland, N. Laing, P.V. Hurse, R.H. Brown Jr., Toxic mutants in Charcot's sclerosis, Nature 378 (1995) 342–343.
[15] L.I. Bruijn, M.K. Houseweart, S. Kato, K.L. Anderson, S.D. Anderson, E. Ohama, A.G. Reaume, R.W. Scott, D.W. Cleveland, Aggregation and motor neuron toxicity of an ALS-linked SOD1 mutant independent from wild-type SOD1, Science 281 (1998) 1851–1854.
[16] J.S. Beckman, M. Carson, C.D. Smith, W.H. Koppenol, ALS, SOD, and peroxynitrite, Nature 364 (1993) 584.
[17] M. Wiedau-Pazos, J.J. Goto, S. Rabizadeh, E.B. Gralla, J.A. Roe, M.K. Lee, J.S. Valentine, D.E. Bredesen, Altered reactivity of superoxide dismutase in familial amyotrophic lateral sclerosis, Science 271 (1996) 515–518.
[18] R.J. Ellis, T.J.T. Pinheiro, Danger-misfolding proteins, Nature 416 (2002) 483–484.
[19] M. Bucciantini, E. Giannoni, F. Chiti, F. Baroni, L. Formigli, J. Zurdo, N. Taddei, G. Ramponi, C.M. Dobson, M. Stefani, Inherent toxicity of aggregates implies a common mechanism for protein misfolding diseases, Nature 416 (2002) 507–511.
[20] D.M. Walsh, I. Klyubin, J.V. Fadeeva, W.K. Cullen, R. Anwyl, M.S. Wolfe, M.J. Rowan, D.J. Selkoe, Naturally secreted oligomers of amyloid beta protein potently inhibit hippocampal long-term potentiation in vivo, Nature 416 (2002) 535–539.
[21] J.A. Johnston, M.J. Dalton, M.E. Gurney, R.R. Kopito, Formation of high-molecular weight complexes of mutant Cu, Zn-superoxide dismutase in a mouse model for familial amyotrophic lateral, Proc. Natl. Acad. Sci. USA 97 (2000) 12571–12576.
[22] S. Mizushima, S. Nagata, pEF-BOS, a powerful mammalian expression vector, Nucleic Acids Res. 18 (1990) 5322.
[23] K. Goto, H. Kondo, A 104-kDa diacylglycerol kinase containing ankyrin-like repeats localizes in the cell nucleus, Proc. Natl. Acad. Sci. USA 93 (1996) 11196–11201.
[24] T. Kato, K. Kurita, T. Seino, T. Kadoya, H. Horie, M. Wada, T. Kawanami, M. Daimon, A. Hirano, Galectin-1 is a component of neurofilamentous lesions in sporadic and familial amyotrophic lateral sclerosis, Biochem. Biophys. Res. Commun. 282 (2001) 166–172.
[25] H.D. Durham, J. Roy, L. Dong, D.A. Figlewicz, Aggregation of mutant Cu/Zn superoxide dismutase proteins in a culture model of ALS, J. Neuropathol. Exp. Neurol. 56 (1997) 523–530.
[26] T. Koide, S. Igarashi, K. Kikugawa, R. Nakano, T. Inuzuka, M. Yamada, H. Takahashi, S. Tsuji, Formation of granular cytoplasmic aggregates in COS7 cells expressing mutant Cu/Zn superoxide dismutase associated with familial amyotrophic lateral sclerosis, Neurosci. Lett. 257 (1998) 29–32.
[27] K. Mori, Tripartite management of unfolded proteins in the endoplasmic reticulum, Cell 101 (2000) 451–454.
[28] T.L. Williamson, D.W. Cleveland, Slowing of axonal transport is a very early event in the toxicity of ALS-linked SOD1 mutants to motor neurons, Nat. Neurosci. 2 (1999) 50–56.
[29] K. Hirano, M. Fukuta, T. Adachi, K. Hayashi, M. Sugiura, Y. Mori, K. Toyoshi, In vitro synthesis of superoxide dismutases of rat liver, Biochem. Biophys. Res. Commun. 129 (1985) 89–94.
[30] L.Y. Chang, J.W. Slot, H.J. Geuze, J.D. Crapo, Molecular immunocytochemistry of the Cu, Zn-superoxide dismutase in rat hepatocytes, J. Cell Biol. 107 (1988) 2169–2179.
[31] J. Nishiyama, Immunoelectron microscopic localization of copper–zinc superoxide dismutase in human gastric mucosa, Acta Histochem. Cytochem. 29 (2002) 215–220.
[32] A. Okado-Matsumoto, I. Fridovich, Subcellular distribution of superoxide dismutases (SOD) in rat liver: Cu, Zn-SOD in mitochondria, J. Biol. Chem. 276 (2001) 38388–38393.
[33] T. Saito, H. Shinzawa, H. Togashi, H. Wakabayashi, K. Ukai, T. Takahashi, M. Ishikawa, M. Dobashi, Y. Imai, Ultrastructural localization of Cu, Zn-SOD in hepatocytes of patients with various liver diseases, Histol. Histopath. 4 (1989) 1–6.
[34] L.A. Sturtz, K. Diekert, L.T. Jensen, R. Lill, V.C. Culotta, A fraction of yeast Cu, Zn-superoxide dismutase and its metallochaperone, CCS, localize to the intermembrane space of mitochondria. A physiological role for SOD1 in guarding against mitochondrial oxidative damage, J. Biol. Chem. 276 (2001) 38084–38089.
[35] J.N. Keller, F.F. Huang, W.R. Markesbery, Decreased levels of proteasome activity and proteasome expression in aging spinal cord, Neuroscience 98 (2000) 149–156.
[36] T. Jin, Y. Gu, G. Zanusso, M. Sy, A. Kumar, M. Cohen, P. Gambetti, N. Singh, The chaperone protein BiP binds to a mutant prion protein and mediates its degradation by the proteasome, J. Biol. Chem. 275 (2000) 38699–38704.
[37] Y. Imai, M. Soda, H. Inoue, N. Hattori, Y. Mizuno, R. Takahashi, An unfolded putative transmembrane polypeptide, which can lead to endoplasmic reticulum stress, is a substrate of Parkin, Cell 105 (2001) 891–902.

Journal of Neuroscience Research 76:265–276 (2004)

Blockade of Interleukin-6 Receptor Suppresses Reactive Astrogliosis and Ameliorates Functional Recovery in Experimental Spinal Cord Injury

S. Okada,[1–3] M. Nakamura,[4] Y. Mikami,[4] T. Shimazaki,[1,3] M. Mihara,[5] Y. Ohsugi,[5] Y. Iwamoto,[2] K. Yoshizaki,[6] T. Kishimoto,[7] Y. Toyama,[4] and H. Okano[1,3]*

[1]Department of Physiology, Keio University School of Medicine, Shinjuku, Tokyo, Japan
[2]Department of Orthopedic Surgery, Graduate School of Medical Sciences, Kyushu University, Fukuoka, Japan
[3]Core Research for Evolutional Science and Technolory (CREST), Japan Science and Technology Agency (JST), Kawaguchi, Saitama, Japan
[4]Department of Orthopedic Surgery, Keio University School of Medicine, Shinjuku, Tokyo, Japan
[5]Chugai Pharmaceutical Company Ltd., Tokyo, Japan
[6]Department of Medical Science I, School of Health and Sport Sciences, Osaka University, Suita, Osaka, Japan
[7]Department of Immunology, Graduate School of Frontier Biosciences Osaka University, Suita, Osaka, Japan

Endogenous neural stem/progenitor cells (NSPCs) have recently been shown to differentiate exclusively into astrocytes, the cells that are involved in glial scar formation after spinal cord injury (SCI). The microenvironment of the spinal cord, especially the inflammatory cytokines that dramatically increase in the acute phase at the injury site, is considered to be an important cause of inhibitory mechanism of neuronal differentiation following SCI. Interleukin-6 (IL-6), which has been demonstrated to induce NSPCs to undergo astrocytic differentiation selectively through the JAK/STAT pathway in vitro, has also been demonstrated to play a critical role as a proinflammatory cytokine and to be associated with secondary tissue damage in SCI. In this study, we assessed the efficacy of rat anti-mouse IL-6 receptor monoclonal antibody (MR16-1) in the treatment of acute SCI in mice. Immediately after contusive SCI with a modified NYU impactor, mice were intraperitoneally injected with a single dose of MR16-1 (100 μg/g body weight), the lesions were assessed histologically, and the functional recovery was evaluated. MR16-1 not only suppressed the astrocytic diffentiation-promoting effect of IL-6 signaling in vitro but inhibited the development of astrogliosis after SCI in vivo. MR16-1 also decreased the number of invading inflammatory cells and the severity of connective tissue scar formation. In addition, we observed significant functional recovery in the mice treated with MR16-1 compared with control mice. These findings suggest that neutralization of IL-6 signaling in the acute phase of SCI represents an attractive option for the treatment of SCI.

Key words: spinal cord injury; IL-6; glial scar; inflammation; neural stem/progenitor cells

Recent studies have shown the existence of neural stem/progenitor cells (NSPCs) in adult mammalian spinal cord and have raised the possibility that the spinal cord has latent capacity for self-repair in response to injury or disease through the use of endogenous NSPCs (Horner et al., 2000; Bjorklund and Lindvall, 2000). After a spinal cord injury (SCI), however, these cells proliferate and migrate to the lesion site, where they differentiate exclusively into astrocytes, never into neurons, and are eventually associated with glial scar formation (Johansson et al., 1999; Takahashi et al., 2003). Glial scar tissue is considered a physical barrier and prevents axonal regeneration by producing axonal growth inhibitors, such as chondroitin sulfate proteoglycans (David and Lacroix, 2003). The major causes of this inhibitory mechanism of neuronal differentiation include the microenvironmental factors that dramatically change immediately following SCI. The interleukin (IL)-6 family of cytokines has been shown to play especially important roles in regulating the various biological responses through multichain receptor complexes-mediated signaling (for review see Taga and Kishimoto, 1997). The multichain receptor complexes, which include the ligand binging receptor (e.g., IL-6-

Contract grant sponsor: Japanese Ministry of Education, Sports and Culture; Contract grant sponsor: Human Frontier Science Program Organization; Contract grant sponsor: Core Research for Evolutional Science and Technology (CREST).

*Correspondence to: Hideyuki Okano, Department of Physiology Keio University School of Medicine, 35 Shinanomachi, Shinjuku, Tokyo, 160-8582, Japan. E-mail: hidokano@sc.itc.keio.ac.jp

Received 8 July 2003; Revised 14 October; Accepted 5 November

Published online 8 March 2004 in Wiley InterScience (www.interscience.wiley.com). DOI: 10.1002/jnr.20044

receptor) and nonligand binding membrane glycoprotein gp130 (Taga et al., 1989), have been shown to play essential roles in signal transduction of the IL-6 family of cytokines. Many lines of evidences suggest that this family of cytokines plays important roles in regulating the immune response (Taga and Kishimoto, 1997), inflammation, and central nervous system (CNS) development and significantly increases in the spinal cord after it is injured (Pan et al., 2002; Nakamura et al., 2003), and gp130-mediated signaling has been demonstrated to induce astrocytic differentiation of NSPCs through the JAK/STAT pathway in vitro (Bonni et al., 1997; Nakashima et al., 1999), suggesting the possibility that blockade of IL-6 trans-signaling after SCI may diminish the reactive astrogliosis and ameliorate functional recovery. Moreover, the IL-6 released during the acute phase of SCI promotes the inflammatory cell chemotaxis and is involved in the secondary injury cascade that is mediated by active inflammatory cell and molecular processes. A recent study has shown that excess activation of gp130 signaling by hyper-IL-6 (a bioactive IL-6/sIL-6R fusion protein) following SCI is associated with a robust inflammatory and glial response that appears to reduce axonal outgrowth in the adult mammalian CNS (Lacroix et al., 2003).

In this study, we used a murine SCI model to investigate the effects of blockade of IL-6 signaling with a monoclonal antibody against the IL-6 receptor (MR16-1, a rat monoclonal antibody that is known to bind to the mouse IL-6-receptor and block the Il-6-mediated cellular responses; Tamura et al., 1993; Takagi et al., 1998; Katsume et al., 2002; Okazaki et al., 2002). We examined whether MR16-1 treatment would offer the promise of a new therapeutic strategy for treating SCI. The results showed that MR16-1 suppressed not only the glial differentiation of NSPCs caused by IL-6 signaling in vitro but also the astrogliosis after SCI in vivo. MR16-1 also decreased infiltration by inflammatory cells and scar tissue formation at the lesion site. In addition, the MR16-1-treated mice showed significantly better functional recovery than the nontreated mice.

MATERIALS AND METHODS

Animals

In total, 74 adult female C57BL/6J mice (18–22 g, 8–10 weeks of age) were used for this study. The ethics committee of our institution approved all surgical interventions and animal care procedures, which were in accordance with the Laboratory Animal Welfare Act, the *Guide for the Care and Use of Laboratory Animals* (National Institutes of Health), and the Guidelines and Policies for Animal Surgery provided by the Animal Study Comittees of the Central Institute for Experimental Animals and of Keio University.

Rat Anti-Mouse IL-6 Receptor Monoclonal Antibody (MR16-1)

The rat anti-mouse IL-6 receptor monoclonal antibody, MR16-1, was prepared as described previously (Tamura et al., 1993). The isotype of this antibody was Ig-G1. MR16-1 was shown to bind to the soluble IL-6 receptor of the mouse and suppress IL-6-induced cellular responses in a dose-dependent fashion (Okazaki et al., 2002). Other basic characterizations of this antibody have been described in previously published reports (Tamura et al., 1993; Okazaki et al., 2002).

Primary Cultures and Passaging Procedures

Spinal cord tissue was dissected from adult mice and transferred into Hank's balanced salt solution (HBSS) containing trypsin (1.33 mg/ml), hyaluronidase (0.67 mg/ml), and kynurenic acid (0.2 mg/ml; all from Sigma, St. Louis, MO) and then minced. After digestion for 4 min at 37°C, the tissue was transferred to HBSS containing trypsin inhibitor (0.7 mg/ml; Roche Diagnostics, Mannheim, Germany) and DNase (0.01 mg/ml; Boehringer Mannheim, Indianapolis, IN). Cells and tissue fragments were washed once with DMEM containing 10% fetal bovine serum (FBS; Hyclone, Logan, UT) and dissociated with a 5-ml pipette. Whole digested tissue was washed again and suspended in DMEM-10% FBS, filtered through sterile 100-mm nylon mesh, and thoroughly mixed with an equal volume of Percoll solution. The cell suspension was fractionated by centrifugation for 30 min, 18°C at 12,300 rpm. Cell fractions were harvested and washed free of Percoll by three rinses in DMEM/10% FBS. After a final centrifugation, the cell suspension was harvested in standard neurosphere culture medium and propagated as described previously (Reynolds and Weiss, 1992; Shimazaki et al., 2001). After the neurosphere-like cell masses had grown to near-confluence, they were passaged and replated at a density of 2×10^5 cells/ml. For differentiation assay, spheres passaged five or six times were dissociated into single cells and plated onto poly-L-ornithine (PO)-coated coverslips at a density of 5×10^5 cells/ml. To investigate the effects of IL-6 signaling on the neural progenitors, we added both IL-6 and soluble IL-6 receptor to the culture medium. As reviewed by Van Wagoner and Benveniste (1999), unlike most soluble receptors that act as antagonists to their respective ligands, the soluble receptor of IL-6 has been shown to function as an agonist of the IL-6-mediated cellular responses by binding to the nonligand binding glycoprotein gp130 (Taga et al., 1989), which acts as a signal transducer of the IL-6 family of cytokines (Taga and Kishimoto, 1997). In the present study, the dissociated adult mouse spinal cord-derived neural precursor cells that had been prepared as described above, were allowed to differentiate for 3 days in the presence of IL-6 (20 ng/ml) and soluble IL-6 receptor-α (sIL-6R; 20 ng/ml), with or w/o MR16-1 (25 μg/ml).

Spinal Cord Injury Model

Female C57BL/6J mice were anesthetized with an intraperitoneal injection of ketamine (100 mg/kg) and xylazine (10 mg/kg). After laminectomy at the T9 level, the dorsal surface of dura matter was exposed. The vertebral column was stabilized with fine forceps and clamps at the T7 and T10 spinous processes and ligament, and the animal's body was then lifted. SCI was induced with a modified NYU impactor (Gruner, 1992; Kuhn and Wrathall, 1998; Jakeman et al., 2000). A 3-g weight (1.2-mm-diameter tip) was allowed to drop from a height of 25 mm onto the dorsal surface of the dura matter. The muscles and the incision were then closed in layers, and the